Salomatov, Vladimir; Kuznetsov, Geniy; Syrodoy, Semen; Gutareva, Nadezhda

Article

Mathematical and physical modeling of the coal-water fuel particle ignition with a liquid film on the surface

Energy Reports

Provided in Cooperation with:
Elsevier

Suggested Citation: Salomatov, Vladimir; Kuznetsov, Geniy; Syrodoy, Semen; Gutareva, Nadezhda (2020) : Mathematical and physical modeling of the coal-water fuel particle ignition with a liquid film on the surface, Energy Reports, ISSN 2352-4847, Elsevier, Amsterdam, Vol. 6, pp. 628-643, https://doi.org/10.1016/j.egyr.2020.02.006

This Version is available at:
https://hdl.handle.net/10419/244064

Energy Reports 6 (2020) 628–643

Contents lists available at ScienceDirect

Energy Reports

journal homepage: www.elsevier.com/locate/egyr

Research paper

Mathematical and physical modeling of the coal–water fuel particle ignition with a liquid film on the surface

Vladimir Salomatov [a], Geniy Kuznetsov [b], Semen Syrodoy [b,*], Nadezhda Gutareva [b]

[a] Kutateladze Institute of Thermophysics SB RAS, Novosibirsk, Russia
[b] National Research Tomsk Polytechnic University, Tomsk, Russia

ARTICLE INFO

Article history:
Received 11 March 2019
Received in revised form 2 December 2019
Accepted 12 February 2020
Available online xxxx

Keywords:
Ignition
Coal-water fuel
Water film
Asymptotic procedures
Particle

ABSTRACT

The results have been presented of the theoretical and experimental research of the ignition processes of single drops of coal–water fuel (CWF). Their surface is covered by a water film. The temperature of the environment T_e has also been recorded and the main characteristics of the process — the times of complete evaporation of the water film (t_{ewf}) and the ignition delays (t_{ign}). The errors in determining T_e have not exceeded 5%.

According to the results of the detailed analysis of the video recordings of the investigated process of ignition, the mathematical models have been developed. They describe the interrelated complex of the thermophysical and thermochemical processes. The approximate analytical solutions of the multistage nonlinear problem of ignition of a coal–water particle have been obtained using the asymptotic procedures.

According to the results of the experimental and theoretical studies, it has been established that the thickness of an aqueous film is one of the parameters determining the conditions and characteristics of the CWF ignition. Moreover, under the conditions of the experiments it has been established that the characteristic evaporation time of the near-surface layer can be from 45 to 60% of the total induction period. They depend on the thickness of the film.

1. Introduction

1.1. Prospects of using coal–water fuel

In the conditions of the constantly changing conjecture on the global markets of hydrocarbons (in particular oil and natural gas), increasing attention is being paid to alternative sources of energy (Demirbas, 2005). Such a situation is connected first and foremost with the fact that it is almost impossible to predict the dynamics of the prices for oil products (Hosseini and Shakouri, 2016; Ghassan and Hajhoj H.R. A.l, 2016). This situation is due to the significantly uneven distribution of the main oil and natural gas reserves on the planet (Penner, 2003). In these circumstances, the countries that possess the reserves of hydrocarbons (Bilgin, 2009), use energy resources as a geopolitical pressure tool (Bilgin, 2005). However, the attempts to replace thermal and nuclear power stations by alternative and renewable energy sources (RES), e.g. wind turbines, solar photovoltaic systems etc., have not been encouraging either today or in the distant future (Sena and Ganguly, 2017). In particular, even in the country's that is most advanced in the use of renewable energy (Germany or Denmark), at the moment, all renewable energy producers would be unprofitable without state subsidies (Andor and Voss, 2016; Strunz et al., 2016). One of the big sources of energy that could compete long-term on the energy market is coal. The supplies of the coal should last for more than 500 years, and they are more evenly distributed across the regions of the world (Thielemann et al., 2007; Rutledge, 2011). Unfortunately, the use of coal as a fuel involves a number of drawbacks, the main ones are high levels of toxic emissions of oxides of nitrogen and sulfur, large output of ash and slags, as well as production of the greenhouse gas, CO2 (Ling et al., 2017).

Designed to date, the systems of environmentally clean burning of coal (for example, using a circulating fluidized bed (Koorneef et al., 2007), the vortex principle (Orlova and Lebedev, 2017), plasma systems (Messerle et al., 2014), etc.) have not been widely applied because of the lack of the scientific support of the above technologies. Among the most promising and environmentally friendly ways of using coal is its combustion in the form of coal–water fuel (CWF) (Longwell et al., 1995). Coal-water fuel is an alternative for replacing pulverized coal as the main fuel in the thermal power plants. CWF is a mixture of coal and water. The ratio of the volume fractions of the components is 50% (water), 49% (coal) and 1% (additives and plasticizers). Accordingly,

* Corresponding author.
E-mail address: ssyrodoy@yandex.ru (S. Syrodoy).

https://doi.org/10.1016/j.egyr.2020.02.006

Abbreviations

Greek letters

α	coefficient of heat transfer W/(m^2 K)
δ	the thickness of the water film
ε	integral degree of blackness
$\theta = \frac{T}{T^*}$	dimensionless temperature;
λ	coefficient of thermal conductivity W/(m K)
ρ	density, kg/m^3
σ	constant of blackbody radiation, W/(m^2 K^4)

Latin letters

a	thermal diffusivity, m^2/s
C	heat capacity, J/(kg K)
L	length scale, m
Q	thermal effect, J/kg
q	heat flow, w/m^2
r	radius, m
t	time, s
T	temperature, K
x_a	thermal perturbation depth, m

Dimensionless criteria

$Bi = \frac{\alpha \cdot L^*}{\lambda}$	dimensionless criterion of Biot
$Fo = \frac{a_{wcf} \cdot t}{(L^*)^2}$	dimensionless criterion of Fourier
$K_\lambda = \frac{\lambda_{dry}}{\lambda_{wcf}}$	a dimensionless heat transfer intensity complex
$K_a = \frac{a_{dry}}{a_{wcf}}$	simplex of nonstationary, a complex characterizing the ratio of the characteristic times of the heating process in the dry and wet parts of the particle
$Ki(Fo) = Bi \cdot (1 - \theta) + Sk \cdot (1 - \theta^4)$	dimensionless criterion of Kirpichev
$M = \frac{Q}{C \cdot T_{eva}}$	dimensionless heat of phase transition
$Sk = \frac{\varepsilon \cdot \sigma \cdot (T^*)^3 \cdot L}{\lambda}$	dimensionless criterion of Stark

Subindexes

0	the initial time
1	dry coal
2	water–coal mixture
e	high temperature gas
w	water
dry	dry coal
ehf	end of process of water film heating
eva	evaporation
ewf	evaporation of water film
fe	full evaporation
hf	process of water film heating
ign	process of ignition
ind	the process of induction of ignition
se	start of evaporation process
shf	start of process of water film heating
st	the initial time
sti	start of process of ignition coal
cwf	coal–water fuel
wf	water film; superscript:* - scale designation

in general, the coal–water fuel can be considered liquid slurry fuel (Cheng et al., 2008). Accordingly, CWF can be sprayed into the combustion chamber with the simple mechanical or pneumatic integral injection nozzles (Beer and Sarofim).

The technology of coal–water fuel has a number of significant advantages compared to the traditional method of burning coal (in the form of pulverized coal or in the fluidized bed). First of all, it is worth noting the significant economic benefit of transportation of coal–water fuel in comparison with coal (Strizhak and Vershinina, 2017). This is due to the fact that CWF can be transported (as from the place of preparation to the thermal power station (TPS)) by pipeline transport (Strizhak and Vershinina, 2017). It is also worth noting that it becomes possible to store CWF in the territory near the TPS in fuel tanks, accordingly, the areas of fuel depots are reduced and the dimensions (sizes) of the fuel supply systems to the burners of the boiler unit are reduced. The in-station space is saved significantly, due to the lack of large fuel bunkers, fuel conveyors and mill equipment.

One of the main advantages of coal–water fuel in comparison with coal is its high ecological compatibility. As established by the authors of Jianzhong et al. (2014), the combustion of coal–water fuel produces a lower level of nitrogen oxides (NOx) than during the combustion of pulverized coal. This is due to the relatively low (T_e <1500 K) combustion temperature of the fuel. It is possible due to the presence of inside pore moisture.

It is also worth noting that earlier it has been experimentally (Jianzhong et al., 2014) and theoretically (Syrodoy et al., 2018) established that when burning coal–water fuel the intensity of formation of slag build-up on the heating surfaces of the combustion device is significantly reduced. This is due to the fact that the combustion temperature of the fuel is substantially lower than the slagging temperature, when CWF is burning, a non-sticky (molten) ash is formed, and a loose, highly porous slag of small thickness that is easily removed by shaking. It has been established (Strizhak and Vershinina, 2017) that under such conditions, even at the relatively low combustion temperature of CWF (T_e <1500 K, for comparison when burning coal 1500 <T_e <2000 K), the intensity of heat transfer through the wall is higher than when burning coal.

A feature that distinguishes CWF from other fuels (coal, biomass) is that it is a slurry fuel containing a large amount of intra-porous moisture. Accordingly, one of the main stages of thermal preparation of fuel for combustion is the process of evaporation of water. It leads to a significantly lower temperature of fuel combustion. This, in turn, leads to a reduction in the formation of NO_x and SO_x oxides but increases the risk of temperature fluctuations and reduces stability of the process of combustion.

1.2. The main problems of implementation of coal–water fuel in power engineering

Today there are a number of the objective reasons significantly hampering the implementation of CWF in the energy sector. One of them is the lack of the developed physical theory and mathematical base, providing a sufficiently high level of confidence in predictive modeling of the thermal processes of preparation and in particular, ignition of the coal–water fuel particles. This is due to the difficulties of modeling of heat transfer in substantially heterogeneous (consisting of different components) structures (CWF). This is due, primarily, to the main and most difficult stage of the thermal preparation of the CWF drop for ignition — water evaporation (Kuznetsov et al., 2015). As has been known from the theory of the phase transformations (Hertz, 1882; Aktershev and Ovchinnikov, 2011a,b), the process of vaporization occurs in a very narrow zone (the evaporation front). For this reason, a

substantially heterogeneous structure is formed in the process of removal of moisture in the CWF particle. The latter consists of a mixture of coal and water (the wet part of the fuel) or a mixture of coal, water vapor, and pyrolysis products. The thermal properties of such a heterogeneous system depend on the location of the evaporation front and are changed abruptly when crossing the border of a phase transition (Syrodoy et al., 2015; Syrodoi et al., 2015; Salomatov et al., 2016). The mathematical modeling is significantly complicated by the fact that during the spraying of coal–water fuel in the combustion chamber, it is highly likely that both partially dried and excessively watered CWF particles will be formed (Murko et al., 2015). This is can be described as a particle, its surface is covered with a water film. As has been established earlier (Zakharevich et al., 2016a), such a liquid layer can have a significant impact on the dynamics of ignition of the CWF particle because of the high endothermic effect of water evaporation (2.5 MJ/kg) and high heat capacity of water (up to 4190 kJ/(kg K)). This may result in the formation of a non-homogeneous (from temperature point of view) structure of the intensive physical and chemical transformations area of CWF, with the presence of relatively cold (in the zone of intensive evaporation of water) and high temperature (more rapid ignition) zones. This is may lead to the flame disruption (Vysokomornaya et al., 2013). It should be noted that the ignition of coal–water fuel particles, the surface of which are coated with a film of water, has not been studied practically under conditions relevant to the combustion space of the boiler units. This is due to the significant technical difficulties of the experimental study when high-temperature video facilities are placed in high-temperature conditions of the real combustion chambers.

But it can be noted that at present no large-scale studies (that at present no large-scale experimental or theoretical studies of the thermal preparation) of the thermal preparation and ignition of coal–water fuel particles coated with a water film have been carried out. This is most likely due to a number of the objective and subjective reasons. For instance, we should mention the fact that the effect of the formation of a water film on the surface of a coal–water particle when spraying CWF in the furnace space has been discovered relatively recently (Murko et al., 2015).

It was discovered three years ago. As for the objective reasons, of course, we should take into account the fact that registration and study of the main stages of the thermal preparation in conditions of a real operation of a typical combustion device are not possible. This is due to the lack of the means for recording the characteristics of the evaporation of the water film and the ignition of the CWF particles against the background of the burning fuel flame because it is practically impossible to establish the means of high-speed video registration in a high-temperature environment. For this reason, in the world scientific periodical literature, with the exception of Zakharevich et al. (2016a), there are no publications devoted to the problem of the water- coal fuel particles ignition coated with a water film.

1.3. A brief overview of the mathematical models of the coal–water fuel particles ignition

Currently, the properties of ignition properties of the particles of a CWF, the surface of which is covered with a water film, are poorly understood. Thus, in Zakharevich et al. (2016a) the results of theoretical and experimental studies of the ignition of the coal–water fuel droplets in the flow of high-temperature gases have been presented. At the same time, investigations have been carried out in a reaction tube into which heated air has been delivered at high speeds (up to 3.8 m/s) and the CWF particle has been suspended on a stationary thermocouple. The speeds of winding in a real combustion device are much lower (no more than 2 m/s) (Wen et al., 2016). Accordingly, it can be assumed reasonably that the application of the results of Zakharevich et al. (2016a) for calculating the combustion chamber of the boiler. It is applicable only for a limited range of the operating conditions of the boiler.

The mathematical model (Zakharevich et al., 2016a) has taken into account the occurrence of the complex of the thermal evolution processes (inert heating, evaporation of the film, dehydration of the main fuel layer, thermal decomposition of the organic part of the fuel) and ignition (oxidation of pyrolysis products) of the CWF drop. It has been established (Zakharevich et al., 2016a) that a water film has a significant effect on the characteristics and the ignition conditions of the coal–water fuel particle. According to the results of the analysis it has been shown that the evaporation of the water film can take up to 60% of the time of the entire induction period. But the experimental studies (Zakharevich et al., 2016a) have been carried out at the relatively low temperatures (up to $T_e \leq 87$ K) of the external environment. It is obvious that such values of T_e do not correspond to the conditions of the combustion chamber spaces of the powerful boiler units (Zhang et al., 2014). In the conditions of high temperatures ($T_e > 1000$ K), the dynamics of the thermal evolution can differ substantially. This is explained by the fact that at $T_e > 1000$ K the thermal radiation becomes intense and the radiative heat flux can be absorbed by the water film not only on the surface, but also in the volume. Accordingly, it can be assumed reasonably that the evaporation characteristics of a water film at $T_e > 1050$ K and $T_e < 900$ K will differ substantially. The effect of absorption of the thermal radiation is taken into account by Syrodoy et al. (Syrodoy et al., 2016b).

Analysis of modern trends in mathematical modeling (Kovenya, 2002) shows that the overwhelming majority of modern researchers prefer numerical methods for solving problems in mathematical physics. But as it has already been mentioned, it requires the use of the energy-intensive computing systems, in some cases of a cluster type. But can be reasonably assumed that the use of supercomputers, for modeling the processes of ignition and combustion of fuel particles in the furnace space, will be quite costly and unreasonable from the economic point of view. This is due to the large-scale variability of the group of factors that have a significant effect on the ignition characteristics of the fuel (ambient temperature, particles size, water film thickness, coal type, particle moisture, degree of fuel grinding, etc.).

For this reason, it is of interest to carry out theoretical studies, the result of which is the development of an approximate analytical solution of the problem of the CWF drop ignition. Such a result creates the prerequisites for the development of a mathematical base for the methodology for calculating the combustion devices with the use of the relatively simple (not petaFLOPs class) electronic computers (Tannehill et al., 1976).

The aim of the work is the experimental investigation of the ignition of coal–water fuel particles, the surface of which is covered with a water film, the formulation of a mathematical model of this process and an approximate analytical solution of the corresponding non-trivial problem, ensuring a sufficiently high predictive potential of the mathematical model.

2. Experiment

2.1. The experiment method

Experimental studies were carried out using the equipment shown in Fig. 1, which is similar to the installation used in the study by Zakharevich et al. (2016b). The fuel particle (coated with a water film) has been fixed on the metal holder and carried in by a remote-controlled coordinate device into the hollow ceramic

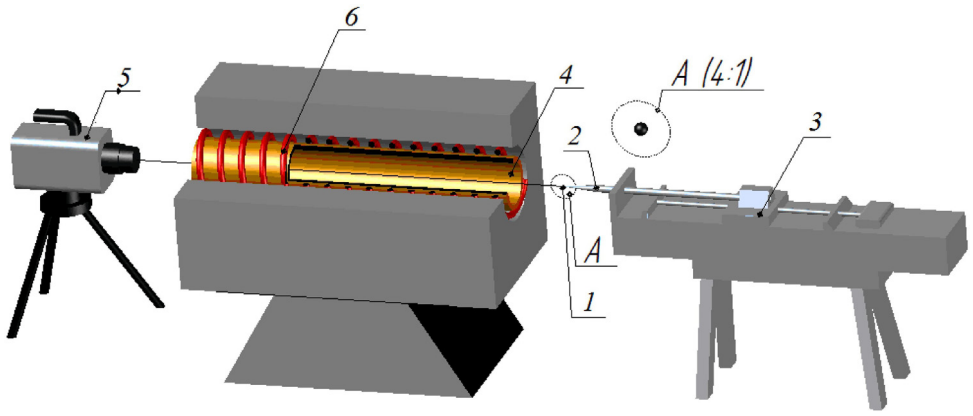

Fig. 1. The experimental setup. 1 — the coal–water particle; 2 — the metal holder; 3 — the coordinate device; 4 — a hollow ceramic tube; 5 — a high-speed video camera; 6 — the electric heater.

cylinder, which has been heated to the temperature $T_e = 1270$ K. The latter has been controlled by chromel-alumel thermocouples (the measurement range $T_e = 300 - 1500$ K). Video recording of the dynamics of the processes of heat and mass transfer and ignition of the CWF particle has been carried out by a high-speed video camera Photron FASTCAM CA4 5 (speed video to 20,000 image/s). The temperature inside the cylinder (T_e) has been varied in a fairly wide range (from 873 K to 1273 K). The period of time from the start of the thermal action (the moment when the fuel particle has been introduced into the cylinder cavity) to the start of the ignition (the flame appearance) has been considered to be the ignition delay time (t_{ign}). The particle sizes have been varied in the range $1.5{\cdot}10^{-3} < \delta < 3.5{\cdot}10^{-3}$ m.

For each external environment temperature, a series of the experiments has been carried out, consisting of 10 experiments. The processing of the experimental data has been carried out using the method of least squares (Amemiya, 1985). The systematic error in determining the main measured parameters (T_e, t_{ign}) has been no more than 5%. In the case of insufficient reliability of the determination of t_{ign}, an additional series of the experiments has been carried out. The confidence interval for determining t_{ign} at a confidence probability of 0.95 has not exceeded 18%.

The software used in the experiments with a high-speed video camera allows you to measure the size of fuel particles. For this reason, the experimental studies on the ignition of particles has been carried out in order to obtain the measurements of the size of the CWF particles (with and without a film). The latter allowed to measure the particle diameters of the CWF particle with a film of water (at the moment of time corresponding to the contact of the particles in the combustion chamber) and after evaporation of the surface water layer. In this case, the thickness of the water layer was calculated by the formula:

$$D = \frac{d_s - d_e}{2};$$

Where: d_s is the particle diameter at the initial moment of time (with a water film on the surface); d_e is the particle diameter at the initial moment of time (without a water layer).

2.2. Characteristics of the fuels

The studies have been carried out for two different types of the coal–water suspension. The first group of CWF has been prepared from the long flame coal of the Kuznetsk basin and the second from the brown coal of the Kansk–Achinsk basin Agroskin and Gleibman (1980).

The studies have been carried out for two different types of the coal–water suspension. The first group of CWF has been prepared from long flame black coal of the Kuznetsk basin and the second from the brown coal of the Kansk–Achinsk basin Agroskin and Gleibman (1980). The preparation of coal–water fuel has been carried out according to the following scheme: a large-sized coal with characteristic stone sizes $d \approx 5{\cdot}10^{-1}$ m has been ground on a stone crusher to the size of pieces $d \approx 2.5{\cdot}10^{-2}$ m in the first stage. The resulting coal crumb has been poured into a ball mill and ground to a particle size of $90 \div 100{\cdot}10^{-6}$ m. If the coal fraction does not match this size, the resulting coal dust has been further ground in the mill. In the next step, the coal dust has been mixed with water (in a recommended proportion of 50/50% by volume) in a homogenizer mixer and brought to a homogeneous state. This ratio in the coal/water system is quite typical in modern

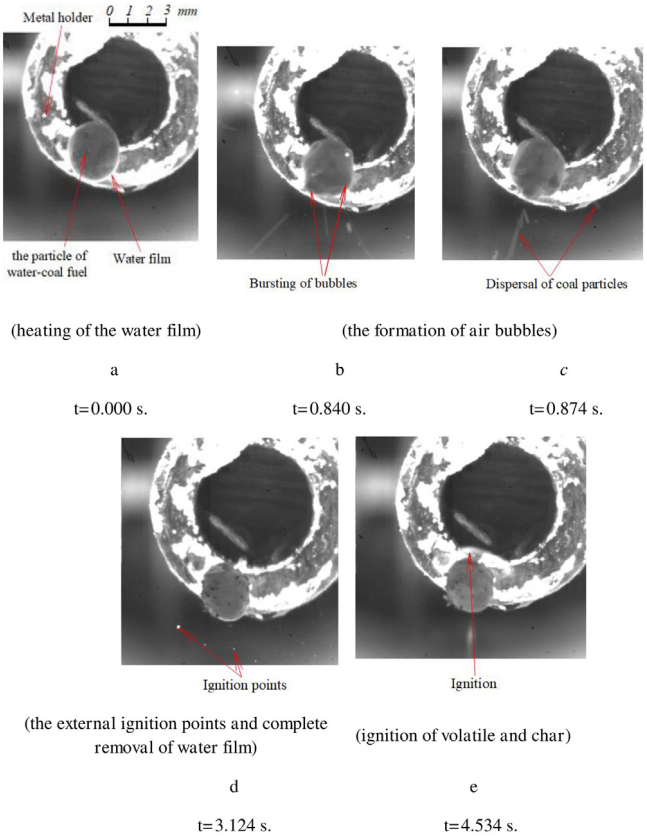

Fig. 2. The typical frames of particle ignition process of coal–water fuel coated water film made from long-flame coal.

energy (Ratafia-Brown et al., 2002; Miller, 2017; Osintsev, 2012; Maltsev et al., 2014; Alekseenko et al., 2019; Svoboda et al., 2012). Accordingly, it can be said that the fuel mixture consisted of water and carbon particles with the characteristic sizes of $d \approx 90 \cdot 10^{-6}$ m. The size of the drops of coal–water drops in the experiment has been varied in a wide range $d = 1.5 \div 3.5 \cdot 10^{-3}$ m. In order to stabilize (prevent the loss of the coal in the solid sediment) in the resulting suspension the additive stabilizer of the type "Nealas" (less than 1%). has been added (Salomatov et al., 2016).

2.3. The results of the experimental studies

Fig. 2 shows frames from a typical videogram of the processes of heating and ignition of the particles (with diameter $d \approx 2.5 \cdot 10^{-3}$ m) of the coal–water fuel, covered with a water film, on the basis of long flame coal at ambient temperature $T_e = 1273$ K. The delay time of ignition $t_{ign} = 4{,}534$ s. The analysis of the videogram shows that the period of the thermal evolution can be divided into several consecutive stages (inert heating, evaporation of water film, the removal of moisture from the base layer of fuel, thermal decomposition and ignition of volatiles, carbon ignition). At the initial moment of time (frame a), the CWF drop, covered with a water film, falls into the high temperature gas environment and is heated. The heating initiates the process of evaporation of the water layer. In the conditions of the ongoing heat exposure (frame b, c) the particle size increases. This is due to the formation of the vapor bubbles inside the film (the transparent areas are seen). This is explained by the fact that under conditions of high-temperature heating water can absorb thermal radiation inside the volume. Analysis of frames b and c shows that the shape of the particle during the heating process (during the time $0.09 \cdot t_{ign} < t < 0.12 \cdot t_{ign}$) undergoes significant changes due to the volumetric boiling of the water film, while we can see the formation of localized points of ignition (frame d) in the outer gas area. This is explained by the fact that the boiling of water and intense vaporization cause the dispersal of the fine carbon particles and their ejection beyond the CWF drop (into the high-temperature oxidizing medium). After a period of time $t \geq 0.7 \cdot t_{ign}$, the water film is evaporated completely (frame d). As a result, a water-particle agglomerate is formed. At $t = t_{ign}$, volatiles are ignited (frame e).

Fig. 3 shows the frames of a typical video of the ignition process of a coal–water drop, coated with a water film, prepared on the basis of brown coal from the Kansk–Achinsk basin. The analysis of the frames shows that the dynamics of the ignition of the CWF particles on the basis of brown coal is similar (in the nature of the main stages) to Fig. 2. However, there are also the significant differences: the brown coal CWF drop is ignited the heating period to full evaporation of the film. It is only about one-third that for coal–water particles made with long-flame coal. This can be explained by the fact that the thermal diffusivity of coal depends essentially on the degree of its metamorphism (a_t of brown coal is less than a_t of long-flame coals). Accordingly, it can be assumed reasonably that in the process of thermal evolution of the drops of brown coal CWF, thermal energy is accumulated in the film much faster than when igniting coal–water particles on the basis of long-flame coal. Also, analyzing the frame b, it can be noted that the boiling of the near-surface water layer in the space around a drop of coal–water fuel the "centers" of ignition in the form of small fragments are formed.

The time characteristics of the thermal evolution processes (evaporation time of the film t_{ewf}) and ignition (delay time of ignition t_{ign}) are shown in Figs. 8–11.

In the remainder of the paper, physical and mathematical models of the process of ignition of the essentially heterogeneous particles of coal–water fuel covered with a water film are formulated on the basis of the detailed analysis of the typical videograms.

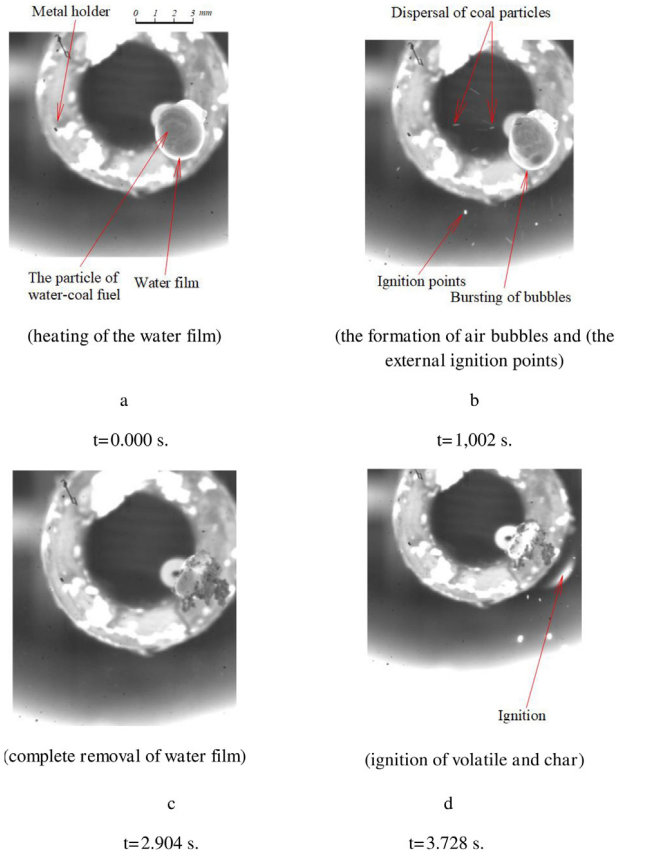

Fig. 3. The typical frames of particle ignition process of coal–water fuel coated water film made from lignite.

3. Physical statement of the problem

At the initial moment of time ($t = 0$), the water-coated CWF particle is introduced into the high-temperature gaseous medium and heated by radiative-convective heat transfer (Fig. 4). As a result, evaporation of the water film is initiated. After the surface layer is removed, a coal–water agglomerate is formed. Its dehydration occurs in the conditions of continuing heating. The evaporation front moves from the surface layers of the fuel to the deep layers. A substantially heterogeneous structure is formed in the particle, consisting of the initial (moisture saturated) fuel and a porous carbon frame with high thermal resistance. Heating of such a fuel leads to an increase in temperature. When the surface temperature, $T(r_{out}, t)$, reaches the critical value, the coal–water fuel particle is ignited.

3.1. Heating of the water film

In the first stage of modeling the ignition of a coal–water particle the processes of heating the near-surface water film have been considered. It is assumed that when a CWF droplet moves in a high-temperature gaseous medium, it warms up to reach the boiling point ($T \approx 373$ K) on the surface of the water film. In formulating the model, the following simplifying assumptions have been adopted:

- the thermophysical properties of the water film are constant;
- the internal convective movements of water in the film are negligible;

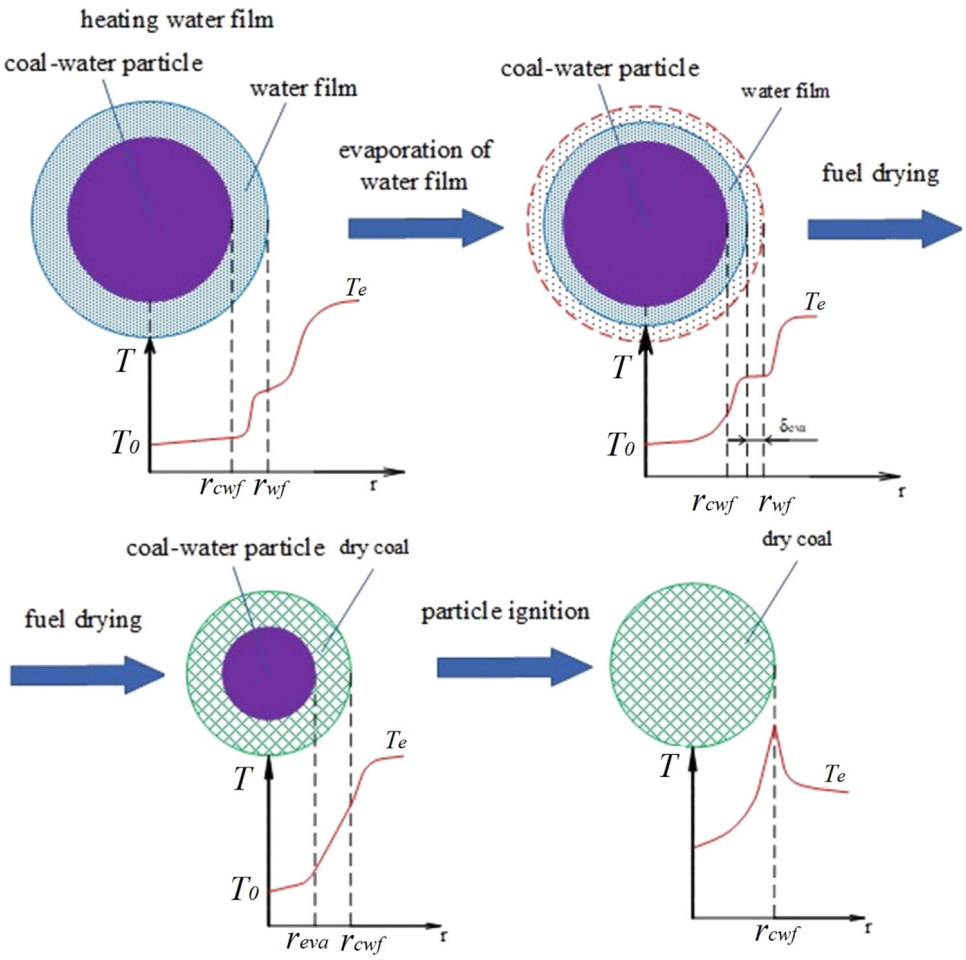

Fig. 4. Scheme for solving the ignition problem.

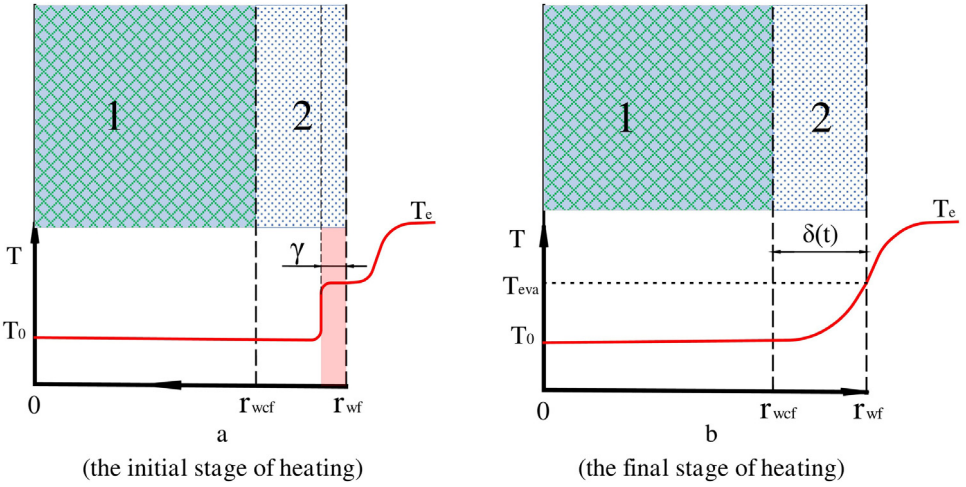

Fig. 5. The scheme of solving the problem of the water film heating. (1 — The particle of coal–water fuel; 2 — water film.)

- the heat exchange with the external environment is due to convection and radiation.

When setting the problem, it has been assumed that the thermal radiation of the external medium is absorbed by a film of water on its surface. The latter can be justified by estimating the length of the free path of the photon (l_f) in the water column. It has been known (Goldstein and Penner, 0000) that the coefficient of molecular absorption of water is $\alpha=1\cdot10^5$ m^{-1} for the spectral range of the waves corresponding to the temperature conditions ($673\leq T_e\leq 1273$ K) of the conducted experiments. Accordingly, the value of the length of the free path of a photon in a water film is $l_f\approx 1/\alpha=1\cdot10^{-5}$ m. Taking into account that the water film thickness $\delta_{wf}=1\cdot10^{-3}$ m, we can say that $l_f \ll \delta_{wf}$, and warm radiation is absorbed on the water surface.

The mathematical formulation of the film heating problem consists of the energy equation for the water film (Carslaw and

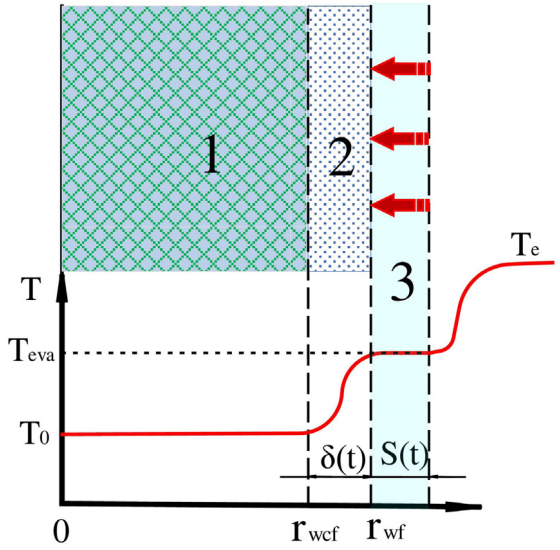

Fig. 6. Scheme of the solution area of the water film evaporation problem. (1 — The particle of coal–water fuel; 2 — water film; 3 — evaporated water layer (steam)); 4 - direction of movement of the water film evaporation front.

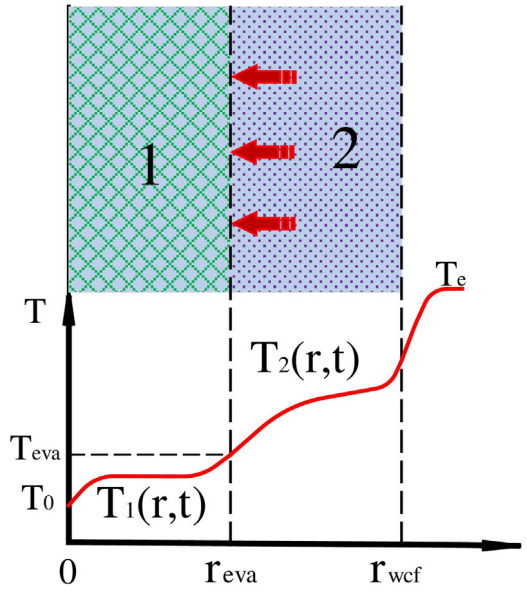

Fig. 7. Scheme of the region for solving the problem of moisture removal. (1 — The particle of coal–water fuel; 2 — dry coal.)

Jaeger, 1959):

$$C_{wf}\rho_{wf}\frac{\partial T}{\partial t}=\frac{\lambda_{wf}}{r^2}\frac{\partial}{\partial r}\left[r^2\cdot\frac{\partial T}{\partial r}\right] \tag{1}$$

$$0<t<t_{se},\ r_{wcf}<r<r_{wf},\ T=T_{se}$$

Eq. (1) has been solved under the following initial and boundary conditions:

$$\left.\frac{\partial T}{\partial r}\right|_{r=r_{wf}}=\frac{\alpha}{\lambda_{wf}}\cdot[T_e-T\,|_{r=r_{wf}}]+\frac{\varepsilon\cdot\sigma}{\lambda_{wf}}\cdot[T_e^4-T^4\,|_{r=r_{wf}}]=q(t)$$

$$0<r<r_{wf},\ T(r,0)=T_0, \tag{2}$$

At the interface of the system "a coal–water particle — a water film", the thermal conjugation condition is fulfilled:

$$\left.\frac{\partial T}{\partial r}\right|_{r=r_{wcf}}=\frac{C_{wcf}\cdot\rho_{wcf}\cdot r_{wcf}}{3\cdot\lambda_{wcf}}\cdot\left.\frac{dT}{dt}\right|_{0<r<r_{wcf}} \tag{3}$$

Here the expression $\left(C_{wcf}\cdot\rho_{wcf}\cdot r_{wcf}\right)/3\cdot\lambda_{wcf}$ determines the absorption of heat by the main fuel layer. When setting the problem, it has been assumed that the temperature gradient along the radius of the main fuel layer (coal–water agglomerate) has been insignificantly affected by the heat transfer characteristics in the water film. This is due to the fact that due to the high (relative to the coal–water agglomerate) heat capacity (4190 J/kg), the water film forms a "barrier" for the heat flow.

Because of the presence of radiant heat transfer, the problem of the film heating is essentially nonlinear and does not have an analytical solution. For this reason, the solution of the water film heating problem is carried out in two stages: the first — the initial (or inertial) stage of heating (Fig. 5a). The second stage is the final (regular, Fig. 5b) heating stage.

3.2. The initial stage of heating

Let us consider the initial stage of heating a water film. The curvature of the water film surface has not been taken into account. To substantiate this assumption, in the formulation of the problem, the numerical studies have been previously carried out to evaluate the influence of the coordinate system used in modeling the processes of thermal conductivity in a coal–water fuel particle with a water film on its surface. The one-dimensional heat conduction problem has been solved for a particle in the form of a sphere and a cubic with the conditions of volume identity. It has been established from the results of numerical simulation that the maximum temperature deviations in the identical heating conditions for two essentially different particles in the range of T to 373 K (the boiling point of water) is less than 0.001 K on the heated surface of the film and less than 5 K at the interface of the system "water coal agglomerate — a film of water". Such results have been obtained for particles of small dimensions (diameter less than 3 mm) that are sufficiently small in the conditions of ambient temperatures of 1000 K.

The process of the film heating is considered using the wave model of thermal conductivity (Marchant, 1993; Salomatov, 1978a) (Fig. 5a). The mathematical model consists of the energy equation for the water film, written in dimensionless variables:

$$\frac{\partial\theta}{\partial Fo}=\frac{\partial^2\theta}{\partial X^2} \tag{4}$$

$$0<Fo<Fo_{se},\ 0<X<1,\ \theta=\theta_{se}$$

$$0<X<1,\ \theta(X,0)=\theta_0,$$

$$\left.\frac{\partial\theta}{\partial X}\right|_{X=0}=\left\{Sk\cdot\left[1-\theta_{X=0}^4(Fo)\right]+Bi\cdot\left[1-\theta_{X=0}^4(Fo)\right]\right\}=Ki(\theta_w,Fo); \tag{5}$$

$$\left.\frac{\partial\theta}{\partial X}\right|_{X=\gamma}=0; \tag{6}$$

$$X=\frac{x}{\delta_{wf}}\quad\theta=\frac{T}{T_e}\quad Fo=\frac{a\cdot t}{\delta_{wf}^2}\quad Bi=\frac{\alpha\cdot\delta_{wf}}{\lambda_{wf}}\quad Sk=\frac{\varepsilon\cdot\sigma\cdot T_e^3\cdot\delta_{wf}}{\lambda_{wf}}$$

Here γ is the thickness of the thermal perturbation zone. The latter can be found from the solution of the equation (Salomatov, 1978a):

$$\gamma(Fo)\simeq\frac{2\cdot[\theta_w(Fo)-\theta_0]}{Ki(\theta_w,Fo)} \tag{7}$$

To solve the non-linear set of Eqs. (4)–(6), we will use the asymptotic method of the thermal quasi stationary approximation developed in Salomatov (1978a). In the initial period of heating the water film, the value of the velocity of the front of the thermal perturbation is determined by the temperature distribution in the water film. Such an assumption is analogous to the condition for a local thermodynamic equilibrium. As a result, the law of the temperature front advance will be formed by these local quasistationary states.

We found the quasi-stationary asymptotic behavior of the boundary value problem (1)–(3) (Salomatov, 1978a). The distribution of the temperature in the film with allowance for three terms of the asymptotic expansion has the form:

$$\theta\,(X, Fo) \simeq \theta_w\,(Fo) + \frac{\gamma\,(Fo)\,Ki\,(\theta_w, Fo)}{2}\left(\frac{X}{\gamma}\right)^2 + \frac{\gamma\,(Fo)\,Ki'\,(\theta_w, Fo)}{2}\left(\frac{X}{\gamma}\right)^2\left[\left(\frac{X}{\gamma}\right)^2 - 2\right] \tag{8}$$

The unknown surface temperature of the water film θ_w(Fo) in (7) and (8) can be find from the solution of the equation:

$$\frac{3}{2}\cdot Sk\cdot Fo \simeq V\left[\theta_w\,(Fo)\,, Fo\right] - V\,(\theta, Fo) \tag{9}$$

$$\begin{aligned} V\,(\theta, Fo) \simeq{}& A_1\cdot\ln(1-\theta) - \frac{A_2}{1-\theta} + B_1\cdot\ln(\theta - b_1) \\ &- \frac{B_2}{\theta - b_1} + \frac{C_1}{2}\cdot\ln\left(\theta^2 + a_2\cdot\theta + b_2\right) \\ &+ \frac{2}{\sqrt{4\cdot b_2 - a_2^2}}\cdot arctg\frac{2\cdot\theta + a_2^2}{\sqrt{4\cdot b_2 - a_2^2}} \\ &\times\left[\left(D_1 - C_1\cdot\frac{a_2^2}{2}\right) + \frac{D_2 - C_2\cdot\frac{a_2^2}{2}}{2\cdot\left(b_2 - \frac{a_2^4}{4}\right)}\right] \\ &+ \frac{\left(D_1 - C_1\cdot\frac{a_2^2}{2}\right)\cdot\left(\theta - \frac{a_2}{2}\right) - C_2\cdot\left(b_2 - \frac{a_1}{4}\right)}{2\cdot\left[1 - \theta^4 + \frac{Bi}{Sk}\cdot(1-\theta)\right]^2} \\ &- \frac{\theta - \theta_0}{C_1\cdot\left[1 - \theta^4 + \frac{Bi}{Sk}\cdot(1-\theta)\right]^2} \end{aligned}$$

Here A_i, B_i, C_i, D_i, a_i, b_i are known constants (Salomatov, 1978a). In the initial stage of the film heating, it is permissible to assume that the surface temperature is low θ_w(Fo) <1, which makes it possible to neglect the back radiation from the surface including the nonlinear term θ_w^4. The last statement is valid for $\theta_w \le 0.65$ (the error in calculating the temperature does not exceed 5%). For these conditions, the asymptotic dependences will have the following form (Salomatov, 1978a):

- the temperature on the surface of the film

$$\theta_w\,(Fo) \simeq \theta_0 + \sqrt{\frac{3}{2}\cdot Sk^2\cdot Fo}\cdot\left(1 + \frac{Bi}{Sk}\right) \tag{10}$$

-the temperature distribution in the water film:

$$\theta\,(X, Fo) \simeq \theta_0 + \sqrt{\frac{3}{2}\cdot Sk^2\cdot Fo}\cdot\left(1 - \frac{X}{\sqrt{6\cdot Fo}}\right)\cdot\left(1 + \frac{Bi}{Sk}\right) \tag{11}$$

-the width of the zone of thermal perturbation:

$$\gamma\,(Fo) \simeq \sqrt{6\cdot Fo} \tag{12}$$

Then the duration of the initial stage of warm-up

$$Fo \simeq \frac{1}{6} \tag{13}$$

Solving Eq. (13), we can find the time (tshf) of the initial stage of the film heating.

3.3. The final stage of the water film heating

Let us consider the second stage of the water film heating — heating to the boiling point (Fig. 5b). Proceeding from the assumption that the main fuel layer (coal–water agglomerate) is a thermally-thin body and applying the procedures of an asymptotic analysis one can obtain an analytical solution of the heating problem. Under these conditions, the mathematical formulation of the problem of a film heating consists of the energy equation for a film:

$$\frac{\partial\theta\,(X, Fo)}{\partial Fo} = \frac{\partial^2\theta\,(X, Fo)}{\partial X^2} \tag{14}$$

$$0 < X < 1;\ \theta\,(X, 0) = \varphi\,(X) \tag{15}$$

At the contact point "water film — coal–water fuel" the following boundary condition is fulfilled:

$$\left.\frac{\partial\theta}{\partial X}\right|_{X=0} = \frac{1}{\xi}\cdot\frac{\partial\rho_{wcf}}{\partial Fo_{wcf}} \tag{16}$$

Here: $\xi = \frac{\lambda_{wf}\cdot C_{wf}\cdot\delta}{\lambda_{wcf}\cdot C_{wcf}\cdot R}$ — the ratio of the accumulating capacities of water and a coal–water suspension.

At the interface "the external environment — a water film", the boundary conditions of the second kind are fulfilled:

$$\begin{aligned} \frac{\partial\theta\,(1, Fo)}{\partial X} = {}& \left\{Sk\cdot\left[1 - \theta_{X=1}^4\,(Fo)\right]\right. \\ &\left. + Bi\cdot\left[1 - \theta_{X=1}\,(Fo)\right]\right\} = Ki\,(Fo)\,; \end{aligned} \tag{17}$$

$$X = \frac{x}{\delta_{wf}} \quad Fo = \frac{a_{wf}\cdot t}{\delta_{wf}^2} \quad Bi = \frac{\alpha\cdot\delta_{wf}}{\lambda_{wf}} \quad Sk = \frac{\varepsilon\cdot\sigma\cdot T_e^3\cdot\delta_{wf}}{\lambda_{wf}}$$

The temperature distribution in such a system is also represented in the form of asymptotic expansion with allowance for two terms by the formula (Salomatov, 1978a):

$$\theta\,(X, Fo) \cong \tilde{\varphi} + \frac{1}{1 + \frac{1}{\xi}}\cdot\left\{\int_0^{Fo} Ki\,(Fo)\,dFo + Ki\,(Fo)\cdot\left[\frac{X^2}{2} + \frac{X}{\xi} - \frac{1 + \frac{3}{\xi}}{6\cdot\left(1 + \frac{1}{\xi}\right)}\right]\right\} \tag{18}$$

Here: $\tilde{\varphi} = \frac{1}{\delta}\int_0^d \varphi\,(x)\,dx$ - is the average temperature in the water film at the moment of the end of the initial warm-up stage

Under the condition X = 1 (18) reduces to an integral equation of Voltaire of the second kind:

$$\begin{aligned} \theta_{wf}\,(Fo) = {}& \tilde{\varphi} + \frac{1}{1 + \frac{1}{\xi}}\cdot\left\{\int_0^{Fo}\left\{Sk\cdot\left[1 - \theta_w^4\,(Fo)\right] + Bi\cdot\left[1 - \theta_w\,(Fo)\right]\right\}dFo\right. \\ &\left. + \left\{Sk\cdot\left[1 - \theta_w^4\,(Fo)\right] + Bi\cdot\left[1 - \theta_w\,(Fo)\right]\right\}\cdot K\,(\xi)\right\} \end{aligned} \tag{19}$$

Here:

$$K\,(\xi) = \frac{1}{3\cdot\left(1 + \frac{1}{\xi}\right)}\cdot\left[1 + \frac{3}{\xi}\cdot\left(1 + \frac{1}{\xi}\right)\right] \tag{20}$$

The integral equation (19) has an analytic solution.

$$Sk\cdot K\,(\xi)\cdot Fo = F\,(\theta) \tag{21}$$

Here:

$$F\,(\theta) = \int_{\tilde{\varphi}}^{\theta_w}\frac{1 + K\,(\xi)\cdot Sk\cdot\left(4\cdot\theta^3 + \frac{Bi}{Sk}\right)}{\left[\left(1 - \theta^4\right) + \frac{Bi}{Sk}\cdot(1 - \theta)\right]}d\theta$$

The temperature distribution in the water film is described by the equation:

$$\theta\,(X, Fo) \simeq \theta_{wf}\,(Fo) - \frac{\left\{Sk \cdot \left[1-\theta_w^4\,(Fo)\right] + Bi \cdot [1-\theta_w\,(Fo)]\right\}}{1+\frac{1}{\xi}} \cdot \left[\frac{1-X^2}{2} + \frac{1-X}{2}\right] \tag{22}$$

Solving Eq. (22) with respect to Fo, we can find the time (t_{ehf}) of the film heating to the boiling point of water (the instant of the stage beginning of water evaporation).

$$t_{hf} = t_{shf} + t_{ehf} \tag{23}$$

3.4. The film evaporation stage

After heating of the water film, the evaporation process is initiated (Fig. 6). The mathematical model of the film evaporation process includes the energy equation:

$$C_{wf}\rho_{wf}\frac{\partial T}{\partial t} = \frac{1}{r^2}\frac{\partial}{\partial r}\left[r^2 \cdot \lambda_{wf} \cdot \frac{\partial T}{\partial r}\right] \quad t > 0, r_{wcf} < r < r_{wf}, T = T_w \tag{24}$$

It is solved with the following initial and boundary conditions:

$$r_{wcf} < r < r_{wf}\,(t)\,, T\,(r, 0) = T_0,$$

$$\left.\frac{\partial T}{\partial r}\right|_{r=r_{wf}} = \frac{\alpha}{\lambda_{wf}} \cdot [T_e - T\,|_{r=r_{wf}}] + \frac{\varepsilon \cdot \sigma}{\lambda_{wf}} \cdot [T_e^4 - T^4\,|_{r=r_{wf}}] - \left.\frac{Q_{ewf} \cdot \rho_{wf}}{\lambda_{wf}} \cdot \frac{d\delta_{wf}\,(t)}{dt}\right|_{r=r_{wf}} \tag{25}$$

$$\left.\frac{\partial T}{\partial r}\right|_{r=r_{wcf}} = \left.\frac{C_{wcf} \cdot \rho_{wcf} \cdot r_{wcf}}{\lambda_{wcf}} \cdot \frac{dT}{dt}\right|_{0<r<r_{wcf}}; \tag{26}$$

In the dimensionless variables, the temperature distribution in the evaporating near-surface water layer, with neglect of its curvature, is described by the equation:

$$\frac{\partial\theta\,(X, Fo)}{\partial Fo} = \frac{\partial^2\theta\,(X, Fo)}{\partial X^2} \quad R\,(Fo) < X < 1 \tag{27}$$

Eq. (27) has been solved under the following boundary conditions:

$$\left.\frac{\partial\theta}{\partial Fo}\right|_{X=1} = \frac{1}{\xi} \cdot \frac{d\theta_{wcf}}{dFo} \tag{28}$$

$$\left.\frac{\partial\theta}{\partial X}\right|_{X=0} = Ki\,(Fo) - V\,(Fo) \tag{29}$$

$$\theta\,(R, Fo)\Big|_{X=0} = 1 \tag{30}$$

$$V\,(Fo) = -M \cdot \dot{R}\,(Fo) \tag{31}$$

Where:

$$M = \frac{Q_{eva}}{C_{wcf} \cdot T_e} \tag{32}$$

$$X = \frac{x}{\delta_{wf}} \quad \theta = \frac{T}{T_{eva}} \quad Fo = \frac{a_{wf} \cdot t}{\delta_{wf}^2}$$

$$Bi = \frac{\alpha \cdot \delta_{wf}}{\lambda_{wf}} \quad Sk = \frac{\varepsilon \cdot \sigma \cdot T_e^3 \cdot \delta_{wf}}{\lambda_{wf}}$$

$$X = \frac{x}{\delta_{wf}} \quad \dot{R}\,(Fo) = \frac{dR_{wf}}{dFo} \quad R_{wcf} = \frac{r_{wcf}}{\delta} \quad T_{eva} = 373\ \mathrm{K}$$

To solve the problem (27)–(32), due to the inherent nonlinearities, the authors (Salomatov, 1978a) have developed an original quasi-stationary approach to the study of the problems with the moving boundaries. It is based on the following physical principle. It is known that the velocity of the boundaries with a phase transition (melting, solidification, evaporation, combustion, formation of a new phase, etc.) is usually much smaller than the rate of the heat pulse transfer. This allows us to use the following approach. The dynamics of the motion of the phase boundary under these conditions will be controlled by the time-limited temperature distributions. We give a decisive role to the quasistationary asymptotics of the temperature field. Using the algorithm for constructing the asymptotic expansions, developed in Salomatov (1978a), we obtain a quasi-stationary approximation, leaving three terms:

$$\theta\,(X, Fo) \simeq \frac{1}{R\,(Fo) + \frac{1}{\xi}} \cdot \left\{\int_0^{Fo} [Ki\,(Fo) - V\,(Fo)]\,dFo + \int_0^{Fo} \varphi\,(X)\,dX + \frac{Ki\,(Fo) - V\,(Fo)}{R\,(Fo) + \frac{1}{\xi}} \cdot \left[\frac{X^2}{2} - \frac{X}{\xi} - \frac{R^2 \cdot \left(R\,(Fo) + \frac{3}{\xi}\right)}{\frac{6 \cdot (R(Fo)+1)}{\xi}}\right]\right\} + \cdots \tag{33}$$

In Eq. (33), the phase boundary of R(Fo) is unknown. If we assume that X = 1 then:

$$\widetilde{\mathrm{Fo}} = \mathrm{N} \cdot [1 - \mathrm{R\,(Fo)}] + \rho\,(1) \cdot \left[1 - \int_0^{\mathrm{Fo}} \frac{\mathrm{dFo}}{\rho\,(\mathrm{R})}\right] \tag{34}$$

$$\widetilde{\mathrm{Fo}} = \frac{1}{\mathrm{Ki\,(0)}} \cdot \int_0^{\mathrm{Fo}} \mathrm{Ki\,(Fo)dFo} \tag{35}$$

where:

$$N = \frac{M}{Ki\,(\theta, Fo)} \tag{36}$$

$$\rho\,(R) = \frac{R\,(Fo)}{3} \cdot \left[R\,(Fo) + \frac{2}{\xi} + \frac{1}{\xi^2} \cdot \frac{1}{R\,(Fo) + \frac{1}{\xi}}\right] \tag{37}$$

Let us consider the initial stage of the film evaporation (R(Fo)→1). In this case, the evaporation time of the film can be calculated by the formula:

$$\widetilde{\mathrm{Fo}} = \mathrm{N} \cdot [1 - \mathrm{R\,(Fo)}] + \rho\,(1) \cdot \left[1\text{-}\exp\left(-\frac{\mathrm{Fo}}{\rho\,(\mathrm{Fo})}\right)\right] \tag{38}$$

The time of a complete evaporation of a water film Fo at R = 0, can be defined as:

$$\mathrm{Fo} = \mathrm{N} - \rho\,(1) \tag{39}$$

The final stage of the film evaporation proceeds under the condition q (Fo) ∼ V (Fo) = 0, respectively, the change in the radius with respect to time can be calculated from:

$$\mathrm{R\,(Fo)} = \frac{\widetilde{\mathrm{Fo}} - \mathrm{Fo}}{\mathrm{N}} \tag{40}$$

In the case q (Fo) = q (0) = const; the numbers $\widetilde{\mathrm{Fo}}$= Fo. Using the formulas (34)–(36), we can determine the total evaporation time of the film t_{ewf}.

3.5. The stage of moisture release

After evaporation of a water film, the water evaporation in the fuel layer is initiated. The evaporation front moves from

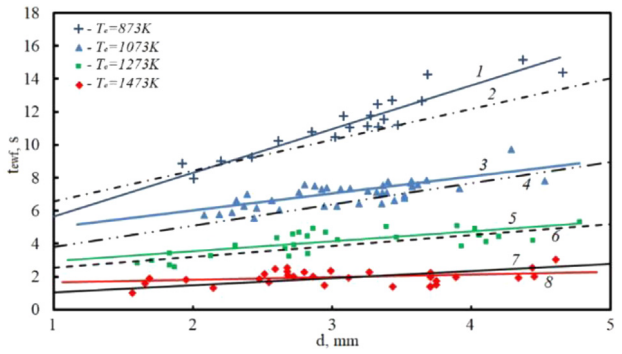

Fig. 8. Dependence of the evaporation time of the water film upon ignition of water–coal particles based on brown coal on the particle diameter. (1, 2 — T_e=873 K; 3, 4 — T_e=1073 K; 5, 6 — T_e=1273 K; 7, 8 — T_e=1473 K; 2, 4, 6, 7 — theoretical solution; 1, 3, 5, 8 — experimental results.)

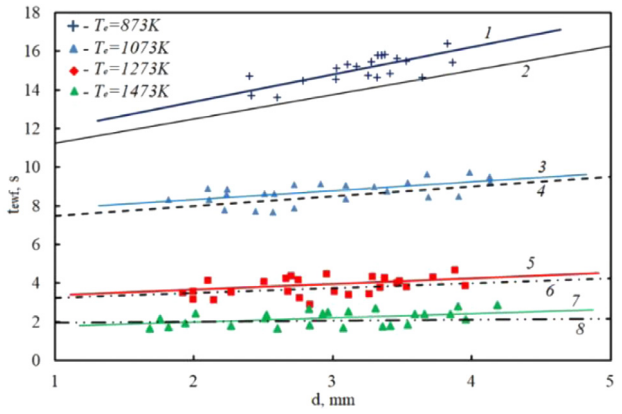

Fig. 9. Dependence of the evaporation time of a water film upon ignition of water–coal particles, based on long-flame coal, on the particle size. (1,2 — T_e=873 K; 3, 4 — T_e =1073 K; 5, 6 — T_e=1273 K; 7, 8 — T_e=1473 K; 2, 4, 6, 8 — theoretical solution; 1, 3, 5, 7 — the results of experiments.)

the surface into the interior of the particle (Fig. 7.). The problem of dehydration of the coal–water fuel particle is considered within the framework of Stefan's conditions (McCord et al., 2016; Dragomirescu et al., 2016). To solve this problem, the method of quasi-stationary approximations, developed in Salomatov (1978b), is used. This is due to the fact that the velocity of the evaporation front is much smaller than the velocity of propagation of the thermal pulse (Salomatov, 1978a). The dynamics of the motion of the front of the phase transition depends on the time-limited temperature distributions in the particle. Accordingly, in order to determine the dynamics of dehydration, it is possible to distinguish quasi-stationary asymptotic. The mathematical statement of the problem of moisture evaporation in a droplet of CWF consists of the system of the nonstationary differential equations of heat conduction describing the temperature distribution in the system "source fuel — dry coal". The temperature field in the dry CWF layer is described by the equation (Salomatov, 1978b):

$$K_a \frac{\partial\theta}{\partial Fo_1} = \frac{\partial^2\theta}{\partial X^2} + \frac{2}{X}\cdot\frac{\partial\theta}{\partial X} \tag{41}$$

$$R_{eva}(Fo) < X < 1; \quad \theta > 1; \quad Fo > Fo_{fe}$$

The temperature distribution in the water-saturated part of CWF is described by the equation:

$$\frac{\partial\theta}{\partial Fo_2} = \frac{\partial^2\theta}{\partial X^2} + \frac{2}{X}\cdot\frac{\partial\theta}{\partial X} \tag{42}$$

$$0 < X < R_{eva}(Fo); \quad \theta_{st} < \theta < 1; \quad Fo > Fo_{fe}$$

The system (41)–(42) has been solved under the following boundary conditions and closing relations:

$$\theta(X,0) = \varphi(X)$$

$$\left.\frac{\partial\theta}{\partial X}\right|_{X=0} = 0 \tag{43}$$

$$\left.\frac{\partial\theta}{\partial X}\right|_{X=1} = Ki(Fo) \tag{44}$$

$$\frac{\partial\theta_1}{\partial X} - K_\lambda\frac{\partial\theta_2}{\partial X} = -M\frac{dR}{dFo} \equiv V(Fo) \tag{45}$$

$$\theta_1(R_{eva}, Fo) = \theta_2(R_{eva}, Fo) \equiv 1 \tag{46}$$

Where:

$$K_a = \frac{a_{dry}}{a_{wcf}} \quad K_\lambda = \frac{\lambda_{dry}}{\lambda_{wcf}} \quad M = \frac{Q_{eva}}{C_2\cdot T_{eva}} \quad \theta = \frac{T}{T_{eva}} \quad T_{eva} = 373\ \text{K}$$

φ(X) — initial distribution of the temperature at the moment of the time of the end of the process of the water film evaporation. K_a — simplex of the nonstationarity process. If K_a <<1 (in other words $\lambda_{dry} \ll \lambda_{cwf}$ or $C_{dry}\cdot\rho_{dry} \gg C_{cwf}\cdot\rho_{cwf}$, the heat conduction process in the initial fuel can be considered stationary. Accordingly, the heat supplied to the moving boundary is expended completely by evaporation. If K_a >>1, it can reasonably be assumed that the heat transfer process in a dry part of the fuel can be regarded as stationary. $K_\lambda = \lambda_{cwf}/\lambda_{dry}$ — complex determining the intensity of the heat flow from the dry to the initial part of the fuel.

Set of Eqs. (41)–(46) belongs to the class of the nonlinear problems with a weak temperature discontinuity at the boundary of the phase transition. To construct its solution, it is necessary to find the time of the onset of evaporation (Fo_{eva}) and the temperature field φ (x). The moment of time Foeva can be found under the condition $\theta_2(Fo_{eva}) = 1$. In this case, evaporation can take place in the initial (for small Fo) or quasistationary (large Fo) stages. As shown by the estimates given in Salomatov (1978b), the boundary of the transition from one stage to another is the inequality Ki≥2. With respect to the case under consideration (the diameter of the CWF droplets d≈1–3·10^{-3} m), it can be reasonably assumed that Ki<2. Then the instant of the onset of evaporation Fo_{eva} and the temperature distribution φ(X) in the drop is determined from the equations:

$$1 - \theta_0 = \int_0^{Fo} Ki(Fo)dFo + \frac{Ki(Fo)}{5} \tag{47}$$

$$\theta_2(X, Fo_{st}) = \varphi(X) = 1 + \frac{Ki(1, Fo_{st})}{2}\cdot(X^2 - 1) \tag{48}$$

Let us distinguish the quasistationary asymptotic in the temperature field for two known φ(X) and Fo_{eva}, taking into account the two terms of the expansion. Under these conditions, the temperature distribution in a dry part of the fuel is calculated by the formula (Salomatov, 1978b):

$$\theta_1(X, Fo) = 1 + \frac{1}{1-R^3}\cdot\left\{3\cdot K_a^{-1}\cdot\int_{Fo_{st}}^{Fo}\left[Ki(\theta_1(1, Fo), Fo) - R^2 q_1(Fo)\right]dFo + \frac{Ki(\theta_1(1, Fo), Fo)}{2}\cdot\left[X^2 - \frac{3}{5} + 2\cdot R^3\cdot W(X, R)\right] - \frac{R^2\cdot q_1(Fo)}{2}\cdot\left[X^2 - \frac{3}{5} + R^2 + 2\cdot W(X, R)\right]\right\}; \tag{49}$$

The temperature distribution in the initial (water-saturated) part of the fuel is described by the formula:

$$\theta_2(X,Fo)=\frac{1}{R^3}\cdot\left\{3\cdot K_a^{-1}\cdot\int_{Fo_{eva}}^{Fo}\left[R^2\cdot(q_1(Fo)-V(Fo))\right]dFo+3\cdot\int_0^R X^2\varphi_2(X)dX+\frac{K_\lambda^{-1}\cdot R^2\cdot[q_1(Fo)-V(Fo)]}{2}\cdot\left(X^2-\frac{3}{5}\cdot R^2\right)\right\} \quad (50)$$

In these conditions: $q_1(\mathrm{Fo})\equiv\partial\theta_1(R,Fo)/\partial X$. The function W (X, R) is a coordinate function. The latter is given in Table 1. The Eq. (50) uses a heat balance conditions:

$$q_1(Fo)-K_\lambda\cdot q_2(Fo)=V(Fo) \quad (51)$$

In the system (49)–(50), we do not know $q_1(Fo)$ and $R(Fo)$. Satisfying the Eqs. (49)–(50) the condition (46), we will obtain the first integral equation:

$$3\cdot K_a^{-1}\cdot\int_{Fo_{st}}^{Fo}\left[Ki(\theta_1,Fo)-R^2\cdot q_1(Fo)\right]dFo=-\frac{Ki(\theta_1,Fo)}{2}\cdot\left[R^2-\frac{3}{5}+2\cdot R^3\cdot W(X,R)\right]+R^2\cdot q_1(Fo)\cdot\left[\frac{R^2}{5}W(X,R)\right]; \quad (52)$$

and the second integro-differential equation:

$$1=\frac{1}{R^3}\cdot\left\{3\cdot K_\lambda-1\cdot\int_0^{Fo}R^2[q_1(Fo)-V(Fo)]dFo+3\cdot\int_0^R X^2\varphi_2(X)dX+\frac{R^3\cdot K_\lambda^{-1}\cdot[q_1(Fo)-V(Fo)]}{5}\right\} \quad (53)$$

Further the time count is from Fo_{eva}. Using (51), Eq. (53) can be written in the form:

$$R^3=3\cdot\int_0^{Fo}R^2\cdot q_2(Fo)dFo+3\cdot\int_0^R x^2\cdot\varphi_2(X)dX+\mathrm{R}^2\frac{q_2(Fo)}{5} \quad (54)$$

The solution (54) has the form:

$$q_2(Fo)=q_2(0)\cdot\mathrm{R}^2\cdot\exp\left[-15\cdot\int 0Fo\frac{dFo}{R^2(Fo)}\right]; \quad (55)$$

where: $q_2\,(0)=Ki\,(Fo_{eva})=Ki(0)$. For the known q2 (0), in order to determine R(Fo), we use (52) with the account of (51) it is converted to the form:

$$3\cdot K_a^{-1}\cdot\int_0^{Fo}\left[Ki(\theta_1,Fo)-R^2(k_\lambda\cdot q_2(Fo)+V(Fo))\right]dFo=\frac{Ki(\theta_{1p},Fo)}{10}\alpha(R_{eva})+\frac{k_\lambda\cdot q_2(Fo)+V(Fo)}{10}\beta(R_{eva}); \quad (56)$$

where

$$\begin{cases}\alpha(R_{eva})=3-5\cdot\left[R^2+2\cdot R^3(Fo)\cdot W(R,R)\right]\\ \beta(R_{eva})=2\cdot R^2\cdot\left[R^2+5\cdot W(R,R)\right]\end{cases}$$

The Eq. (56), describing the dynamics of coal–water fuel dehydration, is presented for a fairly general law of heat exchange. In the case of convective heat transfer, the condition is satisfied on the surface of the CWF drop:

$$\left.\frac{\partial\theta}{\partial X}\right|_{X=1}=Ki(Fo)\equiv Bi\cdot\left(1-\theta\,|_{X=1}\right); \quad (57)$$

In this case, the solution (56) has the form:

$$m\cdot Fo=I_L(R_{eva})+\sum_{i=1}^{2}2I_i(R_{eva})+\sum_{j=1}^{3}P_j(R_{eva}) \quad (58)$$

Where : $\tilde{m}=(\theta_g-1)/M; I_i, P_j$ – known expressions:

$$\sum_{i=1}^{2}I_i\,(R_{eva})=I_1\,(R_{eva})+I_2\,(R_{eva})=\frac{\tilde{m}\cdot K_a}{30}\cdot\Lambda\,(R_{eva})\cdot\Phi\,(R_{eva})+\frac{\tilde{m}\cdot K_a}{10}\cdot\int_1^{R_{eva}}\frac{B\,(R_{eva})}{1-R^3}\cdot F\,(R_{eva})\,dR$$

$$\sum_{i=1}^{3}P_j\,(R_{eva})=P_1\,(R_{eva})+P_2\,(R_{eva})+P_3\,(R_{eva})=\frac{\tilde{m}\cdot K_a\cdot K_\lambda}{30}\cdot[\beta\,(R_{eva})-\alpha\,(R_{eva})\cdot\psi\,(R_{eva})]\cdot\Lambda\,(R_{eva})\cdot q_2\,(R_{eva})+\frac{\tilde{m}\cdot K_a\cdot K_\lambda}{30}\int_1^{R_{eva}}q_2\,(Fo)\cdot\frac{\Psi\,(R_{eva})}{1-R^3}\cdot[\beta\,(R_{eva})-\alpha\,(R_{eva})\cdot\Psi\,(R_{eva})]\,dR+\tilde{m}\cdot K_\lambda\int_0^{Fo}q_2\,(Fo)\cdot\Lambda\,(R_{eva})\cdot\left[\Psi\,(R_{eva})+R^2\right]dFo$$

Here:

$$\Phi(R_{eva})=\frac{\alpha(R_{eva})}{\Lambda(R_{eva})}\cdot[\beta(R_{eva})-\alpha(R_{eva})\cdot\Psi(R_{eva})]\cdot V(R_{eva})$$

$$\Lambda(R_{eva})=\frac{1}{Bi}+\frac{A(R_{eva})}{2}$$

$$\Psi(R_{eva})=\frac{B(R_{eva})}{2\cdot\Lambda(R_{eva})}$$

The first term of Eq. (58) $I_L(R)$ is the solution of Leibenzon (1955):

$$I_L(R)=-\int_1^R A(R)\cdot(R^2+B(R))dR=\frac{1-R}{3}\cdot\left[\frac{1}{Bi}+\frac{A(R)}{2}\right] \quad (59)$$

the second term of Eq. (58) $\sum_{i=1}^{2}I_i(R_{eva})$ – takes into account the overheating of the dried layer; the third $\sum_{i=1}^{3}P_i(R_{eva})$ – heating of the initial (water-saturated) part of the fuel.

The total time of moisture evaporation can be calculated if (58) satisfies condition ($R_{eva}=0$):

$$m\cdot Fo_{fe}=I_L(0)+\sum_{i=1}^{2}(0)+\sum_{j=1}^{3}P_j(0) \quad (60)$$

Solving (60) with respect to Fo, we can determine the time of the complete dehydration of a coal–water particle (t_{fe}). A simpler form of Eq. (60) for calculating the evaporation of moisture dynamics has the following form:

$$\tilde{m}\mathrm{Fo}_{fe}\cong\frac{1}{2}(1-R_u^2)+\frac{1}{3}\left(\frac{1}{Bi}-1\right)\left(1-R_{eva}^3\right)+\frac{\tilde{m}}{10}\left[1-5R_{eva}^2\left(1-\frac{6}{5}R_{eva}\frac{1-R_{eva}^2}{1-R_{eva}^3}\right)\right] \quad (61)$$

3.6. Ignition stage

Let us consider the problem of ignition with the following simplifying assumptions:

- The thermal decomposition of fuel does not have a significant effect on the characteristics of heat transfer.

Table 1
Coordinate functions.

$W(X,R)$	$A(R)=\frac{1-R^2+2\cdot R^3\cdot \Delta W(1,R)}{1-R^3}$	$B(R)=\frac{R^3\cdot(1-R^2-2\cdot\Delta W(1,R))}{1-R^3}$	$\Delta W(X,R)=$ $=W(X,R)-W(R,R)$
$\frac{1}{X}-\frac{9}{5}\cdot\frac{1-R^2}{1-R^3}$	$\frac{2\cdot R^3-3\cdot R^2+1}{1-R^3}$	$R\cdot\frac{R^3-3\cdot R+1}{1-R^3}$	$\frac{R-X}{R\cdot X}$

Table 2
Thermophysical characteristics of the main components of coal–water fuel.

Component of fuel	T, K	λ W/(m · K)	C_p J/(kg · K)	ρ kg/m³	
Subbituminous coal (Long-flame coal)	300	0,116	1150	1285	Agroskin and Gleibman (1980)
	573	0,127	1650		
	773	0,149	1740		
	973	0,173	1790		
	1173	0,207	1830		
	1273	0,243	1850		
Brown coal (lignite)	300	0,145	1150	965	Agroskin and Gleibman (1980)
	573	0,140	1590		
	773	0,168	1740		
	973	0,349	1185		
	1173	0,95	1910		
Water	>373	0,56	4190	1000	
Water vapor	≥373	0,025	2038	0,58	

Table 3
The composition of the coal–water slurry.

	The content of the component coal–water suspension, %		
Type of coal–water fuel	Water	Coal	Additive stabilizer
CWF based on sub-bituminous coal	49	50	1
CWF based on lignite	49	50	1

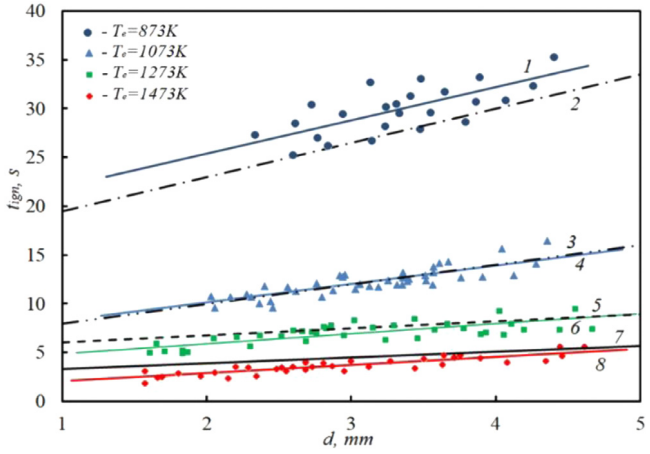

Fig. 10. Dependence of the evaporation time of a water film upon ignition of water–coal particles, based on brown coal, on the particle size. (1, 2 — T_e=873 K; 3, 4 — T_e =1073 K; 5, 6 — T_e=1273 K; 7, 8 — T_e=1473 K; 2, 4, 6, 8 — theoretical solution; 1, 3, 5, 7 — the results of experiments.)

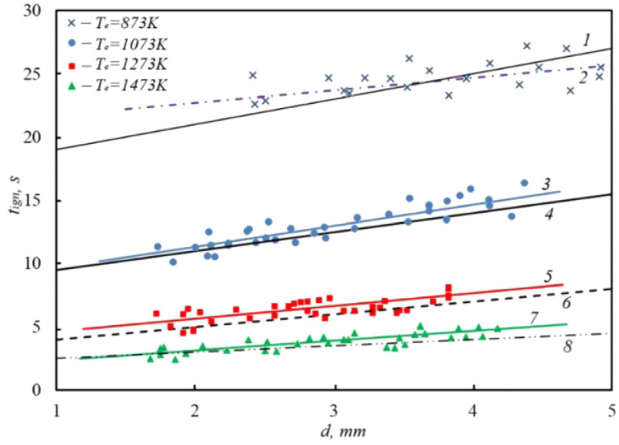

Fig. 11. Dependence of the evaporation times of the water film upon ignition of CWF, on the basis of long-flame coal, on the particle sizes. 1, 2 — T_e=873 K; 3, 4 — T_e=1073 K; 5, 6 — T_e=1273 K; 7, 8 — T_e=1473 K 1, 4, 6, 8 — theoretical solution; 2, 3, 5, 7 — the results of experiments.)

- The thermophysical and thermochemical properties are constant.
- The chemical reaction occurs in a very narrow zone (much smaller than particle size) of the surface can be neglected.

From the theory of thermal explosion (Semenov, 1940), it is known that the initiation of fuel combustion occurs when the critical (fuel surface temperature) ignition conditions are fulfilled. To determine the delay time for the ignition of the CWF particle, we will use the method of the asymptotic approximations developed in Syrodoy et al. (2016a). In particular, the asymptotics of the temperature field (in the dimensionless variables of Frank-Kamenetsky (1987):

$$\theta(0,t)\simeq\frac{\theta_0+(Bi\cdot\theta_0+Ki)\cdot\frac{2\cdot\sqrt{t}}{\sqrt{\pi}}}{1+Bi\cdot\frac{2\cdot\sqrt{t}}{\sqrt{\pi}}} \tag{62}$$

where:

$$\theta=\frac{E}{R\cdot T_{ign}^2}\cdot(T^*-T_{ign})\quad \theta_g=\frac{E}{R\cdot T_{ign}^2}\cdot(T_g-T_{ign})\quad \xi=\frac{X}{X_a};$$

$$\theta_0=\frac{E}{R\cdot T_{ign}^2}\cdot(T_0-T_{ign})\quad Bi=\frac{\alpha\cdot x_a}{\lambda}\quad t_{sti}=\frac{\tau}{\tau_a};$$

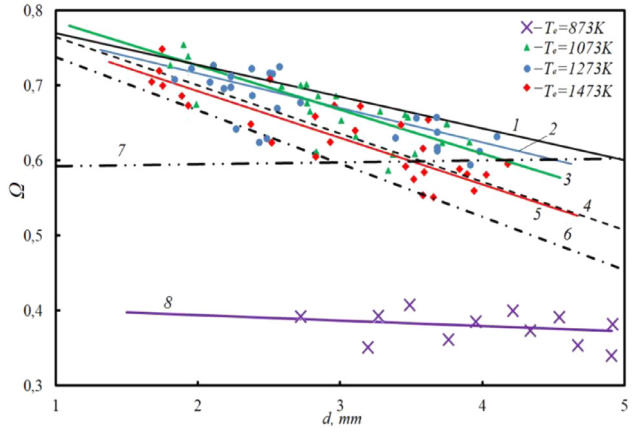

Fig. 12. Dependence of the ratio of the evaporation time of the water film to the ignition delay time on the particle size of the CWF. (Ambient temperature: 7, 8 — T_e=873 K; 1, 3 — T_e=1073 K; 2, 4 — T_e=1273 K; 5, 6 — T_e=1473 K; 1, 4, 6, 7 — theoretical solution; 2, 3, 5, 8 — the results of experiments.)

$$Ki = \frac{E_i}{R \cdot T_{ign}^2} \cdot \frac{x_a}{\lambda_{dry}} \cdot \sigma \cdot \varepsilon \cdot T_e^4 t_a = \frac{R \cdot T_{ign}^2}{E_{ign}} \cdot \frac{C_{dry}}{Q_{ign} \cdot k_{ign}} exp\left(\frac{E_{ign}}{R \cdot T_{ign}}\right) x_a = \sqrt{a \cdot t_a}$$

The dependence (61) at the beginning of the ignition process is converted to the form:

$$\sqrt{\pi \cdot \tau_{si}} \cdot \left(1 + \frac{2}{\pi} \cdot Bi \cdot \sqrt{\tau_{si}}\right)^2 \cdot \exp\left(\frac{\theta_{ign}}{1 + \beta \cdot \theta_{ign}}\right) = Bi \cdot (\theta_g - \theta_0) + Ki \quad (63)$$

If the ignition temperature is taken as the temperature scale T* (in other words, $\theta = 0$), then the expression (63) is transformed to the form:

$$\tau_{sti} = \frac{\pi \cdot \theta_0^2}{4(Bi \cdot \theta_e + Ki)^2} \quad (64)$$

Using the formula (64), it is possible to determine the moment of time of the beginning of the thermochemical reaction of coke carbon with an oxidizer. However, in (64) the unknown is the ignition temperature (θ_{ign}). Substituting the condition (64) into Eq. (52), we will obtain the expression for the calculation of θ_{ign}:

$$\frac{\pi}{2} \cdot \frac{|\theta_{ign}|}{(Bi \cdot \theta_g + Ki)} \cdot \left(1 + \frac{|\theta_{ign}| \cdot Bi}{(Bi \cdot \theta_g + Ki)}\right) = Bi \cdot (\theta_g - \theta_0) + Ki \quad (65)$$

From the solution of O.M. Todes is known (Todes, 1939) that the induction period time can be determined by the formula:

$$t_{ind} = 1 + 2 \cdot \beta \quad (66)$$

Then the total time of ignition delay t_{ign} is calculated by the formula:

$$t_{ign} = t_{hf} + t_{fe} + t_{sti} + t_{ind} \quad (67)$$

3.7. Initial data

A mathematical modeling of the processes of ignition of coal–water fuel particles covered with a water film was carried out for CWF made of typical coals of varying degrees of metamorphism (brown and long-flame). The thermophysical characteristics of the respective components of the fuel are given in Table 2. It was assumed that the thermophysical characteristics of the coal (thermal conductivity, heat capacity, density) do not depend on temperature. The composition of coal–water fuels is given in Table 3. The temporal characteristics of ignition processes were calculated for the experimentally appropriate temperature range (T_e = 873; 1073; 1273 K). The thickness of the water film adopted during the simulation of ignition processes corresponded to the values of δ_{wf} (1–1.5 mm) established in the experiment. The thermophysical characteristics of the coal–water slurry were calculated from the following expressions (Syrodoy et al., 2017):

$$\lambda = \phi_c \lambda_c + \phi_j \lambda_j \quad (68)$$

$$c = \phi_c c_c + \phi_j c_j \quad (69)$$

$$\rho = \phi_c \rho_c + \phi_j \rho_j \quad (70)$$

Where j – w for a wet particle of CWF; j – s for the dried particle; ϕ is the volume fraction of the coal–water slurry component.

4. Results and their discussion

4.1. Evaporation of a water film

Fig. 8 shows the results of the theoretical and experimental studies of the process of evaporation of a water film upon ignition of the CWF particle based on the brown coal under conditions corresponding to the combustion chambers of the boiler units. The analysis of the curves (1)–(6) shows that the evaporation times of the film at the external temperatures T_e = 1273 K differ from t_{ewf} at T_e = 1073 K negligibly (the relative deviation $\delta t \leq 10\%$).

This is due to the fact that under the conditions of high-temperature heating (T_e > 1073 K) the radiative component of the heat flux is significant in comparison with the convective one. For this reason, the heating of the film occurs much faster than the evaporation of water. In this case, the analysis of the curves in Fig. 8 shows that, under conditions of high temperatures of the external medium, the particle size has little effect on the evaporation dynamics. This can be explained by the fact that in the general case the suspension part of the CWF drop is thermally thin compared with the water film. At relatively low the ambient temperatures ($T_e \leq 800$ K), evaporation of the water film takes much longer.

Fig. 8 also shows the results of the theoretical studies of the evaporation of a water film under conditions corresponding to the furnace space of the boiler units. It can be noted that the calculated evaporation times are satisfactory (within the confidence interval) consistent with the experimental data.

Fig. 9 shows the evaporation times of the water film in the event of ignition of coal–water particles based on long-flame coal. Analyzing the results, it can be concluded that, under relatively low temperatures ($T_e \leq 873$ K) of the external environment, the dynamics of evaporation differs significantly from the evaporation of the water layer at $T_e \geq 1073$ K. Fig. 9 also shows theoretically calculated evaporation times of a water film. The obtained dependences show sufficient agreement between the theoretical and experimental results. The deviation of the values t_{ewf} does not exceed 8%.

The comparative analysis of Figs. 8 and 9 shows that the evaporation of the water film in the case of ignition of the brown coal particles of CWF occurs much faster than when igniting coal–water droplets based on the long-flame coal. This can be explained by the significantly higher thermal resistance of brown coal compared to the long-flame coal. Accordingly, under conditions of intense thermal impact of the external environment, the accumulation of thermal energy in the water film of the brown coal droplets of CWF occurs much faster than when ignition of the coal–water particles made from long-flame coal.

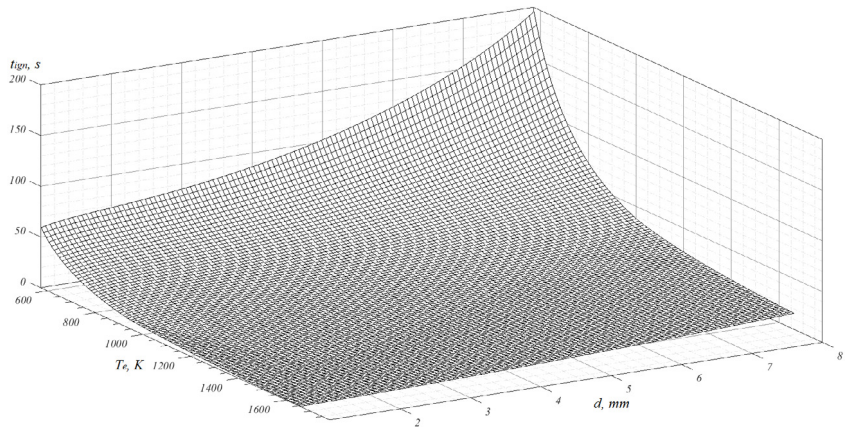

Fig. 13. Dependence of ignition delay times of coal–water fuel particles covered with a water film (thickness $\delta = 1$ mm), on the temperature of the external medium and the diameter of the particle.

4.2. Ignition of coal–water fuel particle

Fig. 10 shows the dependences of the ignition delay times of coal–water fuel particles based on the brown coal covered with a water film, under conditions corresponding to the furnace areas of the boiler units.

The analysis of the results shows that with high-temperature heating ($T_e > 873$ K), the duration of the evaporation process of a water film can be up to 60% of the total induction period. This is primarily due to the fact that in the conditions of intense heating the boiling of water begins. As a result, the main fuel layer is heated to the temperatures close to the boiling point ($\sim$ 373 K). Accordingly, the subsequent moisture removal proceeds much faster. The latter correlates with the results of Zakharevich et al. (2016a). This correlation confirms indirectly the hypothesis that in the process of thermal evolution of fuel for ignition, the coal–water part of the CWF drop is a thermally thin body.

Other essential regularities have been established at ignition of the coal–water particles at rather low temperatures of an environment ($T_e \leq 873$ K). The evaporation time of the film is less than 50% of t_{ign}. As it has been mentioned earlier, this can be explained by the fact that under conditions of the relatively low temperatures of the external environment, the intensity of the heat flux is small and does not significantly affect the heating rate of the CWF particle (due to intensive evaporation of the water film). Fig. 8 also shows theoretically calculated values of t_{ign}. It can be noted that in the region of high temperatures of the external environment, the deviations of the theoretical values of the ignition delay times from the experimental values do not exceed 5%.

Another situation with $T_e \leq 873$ K is that the deviations of the theoretical and experimental results are significant, but still do not exceed 15%.

Fig. 11 shows the experimental and theoretical dependences of t_{ign} on the CWF particle size based on the long-flame coal, the surface of which is covered with a water film. The analysis of the results makes it possible (as in Fig. 8) to draw a conclusion about the effect of the water layer on the characteristics and conditions of ignition. The comparative analysis of Figs. 10 and 11 shows that the brown coal particles of CWF are ignited much faster than fuel drops based on the long-flame coal. All the calculated values of ignition delay times are in satisfactory agreement with the experiment.

Fig. 12 shows the ratio of the evaporation time of the water film to the ignition delay time ($\Omega = t_{ewf}/t_{ign}$), depending on the size of the coal–water fuel particle at various ambient temperatures. It can be noted that practically in the entire temperature range of the external environment, t_{ewf} is up to 60% (by experimental values) and up to 70% according to theoretically calculated data from the entire ignition delay. This is due to the fact that during the time of evaporation of the water film, the heating of the main fuel layer occurs. As a result, evaporation of the intraporous moisture and ignition proceeds more quickly than when the particle is ignited without a water film.

It should also be noted that at relatively low ambient temperatures ($T_e \leq 873$ K), the value of $\Omega \approx 0.5$. This is due to the increase in the total period of heat treatment (evaporation of the water film and the pore moisture), and ignition in consequence of the high cost of energy on the processes of phase transition and initiation of combustion of a fuel.

4.3. Applicability of the results

After verification (comparisons of the theoretical and experimental values of ignition delay times) of the mathematical model, it is possible to carry out a prognostic modeling of the processes of ignition of a coal–water fuel particle covered with a water film. The obtained approximate-analytical solution of the problem can be easily realized in the Matlab18b environment.

Fig. 13 shows the field of the ignition delay times of the coal–water fuel particle when the dimensions of the fuel particle and the temperature of the external medium (T_e) changed, which were varied over a fairly wide range: d = 1–8 mm and $T_e = 673 \div 1673$ K. 1110^4 variants of combinations d and T_e were analyzed. The calculation time was 1054 s. A numerical simulation of the processes of ignition of the CWF drop (one combination of d and T_e) with the use of the modern software packages, as a rule, takes 5 to 48 h. The analysis of the dependences t_{ign} (d, T_e) shows that with increasing d and decreasing T_e, the delays of ignition substantially increase. For example, for d = 8 mm and $T_e = 4$ 673 K, the calculated value $t_{ign} \approx 140$ s. Most likely this means that particle ignition at such values of d and T_e will not occur.

In conclusion, we can say that the approximate analytical solution of the problem of ignition of a coal–water fuel particle covered with a water film obtained by the authors of the article can be used in the prognostic modeling of thermal preparation and ignition of CWF drops under conditions corresponding to the combustion chambers of the perspective coal–water boiler units. With the use of computers it is possible to carry out large-scale calculations that will allow choosing the most effective parameters of the combustion chambers of the boiler units (the size of the combustion chamber, the temperature regime of the combustion chamber and burner devices, the rate of oxidant supply).

On the whole, it can be concluded that the approximate analytical solution of the essentially non-linear problem of ignition of coal–water fuel particles (the surface of which is covered with a water film), obtained (as a result of the studies carried out in this work aimed at solving an actual problem of great fundamental, engineering and economic importance) is an objective basis for a significant reduction in the expenditure of time (up to 10,000 times) on the modeling of work and the choice of design parameters of the combustion chambers of the new perspective fuel compositions.

4.4. Conclusion

According to the results of theoretical and experimental studies, the main time characteristics of the thermal evolution processes (the evaporation time of the water film) and the ignition (the ignition delay time) of the coal–water fuel particles whose surface is covered with a thin water layer have been established. The drops of the fuels based on coals of various degrees of metamorphism (the brown and long-flame) have been investigated. The laws of thermal evolution and ignition of the CWF particles coated with a water film under conditions of high ambient temperatures ($T_e > 1000$ K) have been studied for the first time. It has been established that the evaporation of the near-surface water film has a significant effect on the characteristics and conditions of ignition. Thus, the film evaporation time can take up to 60% of the total induction period. This is correlated fairly accurately with the experimental results (Zakharevich et al., 2016a). When the water film evaporates, the main fuel layer is also warmed up to the boiling point. As a result, the subsequent dehydration of the main fuel layer occurs much faster.

As a result of the experimental and theoretical studies of the ignition of drops of coal–water fuel, the surface of which is covered with the water film, it has been established that the ignition delay times (t_{ign}) of such fuels are up to 30 s. Such values of t_{ign} create the prerequisites for the emergence of risks of non-ignition of fuel in the combustion chamber, using the "classical" Π-formed chamber furnaces (Xin et al., 2018). Accordingly, for the stable ignition of coal–water fuel particles, the combustion device must be arranged in the form of two combustion chambers: there is the thermal preparation of the fuel for combustion (evaporation of the water film, removal of moisture from the main fuel layer, ignition) in the first chamber, there is the direct combustion and heat transfer to the combustion walls in the second one. Such a combustion mode is provided by using the so-called cyclone (vertical or horizontal) pre-firing devices (Boysan et al., 1986), in which the ignition is carried out.

According to the results of the detailed analysis of the videograms, it has been established that the period of thermal evolution and ignition of the coal–water fuel particle coated with a water film consists of a number of the separate interrelated processes (heating and evaporation of the water film, dehydration of the main fuel layer, ignition of volatiles and coke). As a result, a mathematical model describing all the stages of thermal evolution and fuel ignition has been developed. An analytical solution of the nonlinear ignition problem has been obtained for the first time with using the asymptotic analysis procedures. The comparison of the theoretical values of the evaporation times of the film and the delays of ignition with the experimental data has shown their quite satisfactory conformity. This shows that the obtained analytical solution of the ignition problem allows to carry out at a sufficiently high level the reliable predictive modeling of the ignition processes of the essentially non-uniform drops of CWF covered with a water film. It can also be said that the approximate-analytical solution of the problem that has been obtained during the experiments allows a substantial reduction in the time and material resources in the analysis of the ignition of the CWF particles with using a computer.

The developed analytical solutions of the mechanism of the CWF ignition can become the basis for design of the coal–water combustion chambers.

Declaration of competing interest

The authors declare that they have no known competing financial interests or personal relationships that could have appeared to influence the work reported in this paper.

CRediT authorship contribution statement

Vladimir Salomatov: Methodology, Formal analysis. **Geniy Kuznetsov:** Conceptualization, Writing - review & editing. **Semen Syrodoy:** Methodology, Software, Project administration. **Nadezhda Gutareva:** Writing - original draft.

Acknowledgment

This work is supported by the Russian Science Foundation under grant 18-79-10015

Appendix A. Supplementary data

Supplementary material related to this article can be found online at https://doi.org/10.1016/j.egyr.2020.02.006.

References

Agroskin, A.A., Gleibman, V.B., 1980. Thermal Physics of Solid Fuel. Moscow.
Aktershev, S.P., Ovchinnikov, V.V., 2011a. The boiling up model for highly superheated liquid with formation of evaporation front. Thermophys. Aeromech. 18, 591–602.
Aktershev, S.P., Ovchinnikov, V.V., 2011b. Modeling of the vaporization front on a heater surface. J. Eng. Thermophys. (20), 77–88.
Alekseenko, S.V., Kuznetsov, V.A., Mal'tsev, L.I., Dekterev, A.A., Chernetskii, M.Yu., 2019. Analysis of combustion of coal-water fuel in low-power hot-water boiler via numerical modeling and experiments. J. Eng. Thermophys. 28, 177–186.
Amemiya, T., 1985. Advanced Econometrics. Harvard University Press.
Andor, M., Voss, A., 2016. Optimal renewable-energy promotion: Capacity subsidies vs. generation subsidies. Resour. Energy Econ. 45, 144–158.
Beer, J.M., Sarofim, A.F., Fundamental Aspects of Coal-Water Fuel Droplet Combustion and Secondary Atomization of Coal-Water Mixtures. Final Reports, The Energy Laboratory and Department of Chemical Engineering Massachusetts Institute of Technology Cambridge, Massachusetts, 02139.
Bilgin, M., 2005. Eurasian Energy Wars. IQ Publishing, Istanbul.
Bilgin, M., 2009. Geopolitics of european natural gas demand: Supplies from Russia, Caspian and the Middle East. Energy Policy 37, 4482–4492.
Boysan, F., Weber, R., Swithenbank, J., 1986. Modeling coal-fired cyclone combustors. Combust. Flame 63, 73–86.
Carslaw, H., Jaeger, J., 1959. Conduction of Heat in Solids, second ed. Oxford University Press, USA, p. 510.
Cheng, J., Zhou, J.H., Li, Y.C., Liu, J.Z., Cen, K.F., 2008. Effects of pore fractal structures of ultrafine coal water slurries on rheological behaviors and combustion dynamics. Fuel 87, 2620–2627.
Demirbas, A., 2005. Potential applications of renewable energy sources, biomass combustion problems in boiler power systems and combustion related environmental issues. Prog. Energy Combust. Sci. 31, 171–192.
Dragomirescu, F.I., Eisenschmidt, K., Rohde, C., Weig, B., 2016. Perturbation solutions for the finite radially symmetric stefan problem. Int. J. Therm. Sci. 104, 386–395.
Frank-Kamenetsky, D.A., 1987. Diffusion and Heat Transfer in Chemical Kinetics. Nauka, Moscow.
Ghassan, H.B., Hajhoj H.R. A.l, 2016. Long run dynamic volatilities between OPEC and non-OPEC crude oil prices. Appl. Energy 169, 384–394.
Goldstein, R., Penner, S.S., 0000. The Near-Infrared Absorption to Liquid Water at Temperatures between 27 and 209 0C. J. Quant. Spectry. Radiat. Transf. 4. 441–451.
Hertz, H., 1882. On the evaporation of liquids, especially mercury, in vacuo. Ann. Physics 17, 12.

Hosseini, S.H., Shakouri, H., 2016. A study on the future of unconventional oil development under different oil price scenarios: A system dynamics approach. Energy Policy 91, 64–74.
Jianzhong, Liu, Ruikun, Wang, Jianfei, Xi, Junhu, Zhou, Kefa, Cen, 2014. Pilot-scale investigation on slurrying, combustion, and slagging characteristics of coal slurry fuel prepared using industrial waste liquid. Appl. Energy 115, 309–319.
Koornneef, J., Junginger, M., Faaij, A., 2007. Development of fluidized bed combustion—An overview of trends, performance and cost. Prog. Energy Combust. Sci. 33, 19–55.
Kovenya, V.M., 2002. Problems and trends in mathematical modeling. J. Appl. Mech. Tech. Phys. 43, 345–353.
Kuznetsov, G.V., Salomatov, V.V., Syrodoy, S.V., 2015. Numerical simulation of ignition of particles of a coal–water fuel. Combust. Explos. Shock Waves 51, 409–415.
Leibenzon, L.S., 1955. Collection of Scientists. Nauka, Moscow.
Ling, Zhongqian, Ling, Bo, Kuang, Min, Li, Zhengqi, Lu, Ye, 2017. Comparison of airflow, coal combustion, NOx emissions, and slagging characteristics among three large-scale MBEL down-fired boilers manufactured at different times. Appl. Energy 187, 689–705.
Longwell, J.P., Rubin, E.S., Wilson, J., 1995. Coal: Energy for the future. Prog. Energy Combust. Sci. 21, 269–360.
Maltsev, L.I., Kravchenko, I.V., Lazarev, S.I., Lapin, D.A., 2014. Combustion of black coal in the form of coal–water slurry in lowCapacity boilers. Therm. Eng. 61, 486–490.
Marchant, T.R., 1993. Thermal waves for nonlinear hyperbolic heat conduction. Math. Comput. Model. 18, 111–121.
McCord, D., Crepeau, J., Siahpush, A., Angelo, J., Brogin, F., 2016. Analytical solutions to the stefan problem with internal heat generation. Appl. Therm. Eng. 103, 443–451.
Messerle, V.E., Karpenko, E.I., Ustimenko, A.B., 2014. Plasma assisted power coal combustion in the furnace of utility boiler: Numerical modeling and full-scale test. Fuel 126, 294–300.
Miller, B.G., 2017. Clean Coal Engineering Technology. The Pennsylvania State University, Pennsylvania.
Murko, V.I., Fedyaev, V.I., Karpenok, V.I., Senchurova, Y.A., Riesterer, A., 2015. Investigation of the spraying mechanism and combustion of the suspended coal fuel. Therm. Sci. 19, 243–251.
Orlova, K.Y., Lebedev, B.V., 2017. Research of power fuel low-temperature vortex combustion in industrial boiler based on numerical modelling. MATEC Web Conf. 92, 01003.
Osintsev, K.V., 2012. Studying flame combustion of coal–water slurries in the furnaces of powergenerating boilers. Therm. Eng. 59, 881.
Penner, S.S., 2003. Energy Resources and Reserves. Encyclopedia of Physical Science and Technology, third ed. pp. 461–476.
Ratafia-Brown, J., Manfredo, L., Hoffman, J., Ramezan, M., 2002. Major Environmental Aspects of Gasification-Based Power Generation Technologies. Office of Fossil Energy.
Rutledge, D., 2011. Estimating long-term world coal production with logit and probit transforms. Int. J. Coal Geol. 85, 23–33.
Salomatov, V.V., 1978a. Methods for calculating nonlinear heat transfer processes. Part 1e. From TSU. Tomsk.
Salomatov, V.V., 1978b. Methods for calculating nonlinear heat transfer processes. Part 2. From the TSU. Tomsk.
Salomatov, V.V., Kuznetsov, G.V., Syrodoy, S.V., Gutareva, N.Y., 2016. Ignition of coal-water fuel particles under the conditions of intense heat. Appl. Therm. Eng. 106, 561–569.
Semenov, N.N., 1940. Thermal theory of combustion and explosion. Adv. Phys. Sci. T.XXIII 3, 251–592.
Sena, S., Ganguly, S., 2017. Opportunities, barriers and issues with renewable energy development – A discussion. Renew. Sustain. Energy Rev. 69, 1170–1181.
Strizhak, Pavel A., Vershinina, Ksenia Yu., 2017. Maximum combustion temperature for coal-water slurry containing petrochemicals. Energy 120, 34–46.
Strunz, S., Gawel, E., Lehmann, P., 2016. The political economy of renewable energy policies in Germany and the EU. Util. Policy 42, 33–41.
Svoboda, K., Pohorelý, M., Jeremiáö, M., Kamení ková, P., Hartman, M., Skoblja, S., äyc, M., 2012. Fluidized bed gasification of coal–oil and coal–water–oil slurries by oxygen–steam and oxygen–CO2 mixtures. Fuel Process. Technol. 95, 16–26.
Syrodoi, S.V., Kuznetsov, G.V., Salomatov, V.V., 2015. Effect of the shape particles of the characteristics of the ignition of coal-water fuel. Solid Fuel Chem. 49, 409–415.
Syrodoy, S.V., Gutareva, N.Y., Salomatov, V.V., 2016a. Initiation of ignition of highly fuel particles in the flow of high temperature medium. EPJ Web Conf. 110, 01023.
Syrodoy, S.V., Gutareva, N.Y., Taburchinov, R.I., 2016b. Influence of absorption of thermal radiation in the surface water film on the characteristics and ignition conditions. MATEC Web Conf. 72, 01109.
Syrodoy, S.V., Kuznetsov, G.V., Gutareva, N.Y., Salomatov, V.V., 2018. The efficiency of heat transfer through the ash deposits on the heat exchange surfaces by burning coal and coal-water fuels. J. Energy Inst. 91, 1091–1101.
Syrodoy, S.V., Kuznetsov, G.V., Salomatov, V.V., 2015. The influence of heat transfer conditions on the parameters characterizing the ignition of coal-water fuel particles. Therm. Eng. 62, 703–707.
Syrodoy, S.V., Kuznetsov, G.V., Zhakharevich, A.V., Gutareva, N.Y., Salomatov, V.V., 2017. The influence of the structure heterogeneity on the characteristics and conditions of the coal–water fuel particles ignition in high temperature environment. Combust. Flame 180, 196–206.
Tannehill, J.C., Anderson, D.A., Pletcher, R.H., 1976. Computational Fluid Mechanics and Heat Transfer. Hemisphere Publishing, p. 599.
Thielemann, T., Schmidt, S., Gerling, J.P., 2007. Lignite and hard coal: Energy suppliers for world needs until the year 2100 — An outlook. Int. J. Coal Geol. 72, 1–14.
Todes, O.M., 1939. The theory of thermal explosion. I. Thermal explosion reaction of zero order. Russian J. Phys. Chem. A 13, 868–879.
Vysokomornaya, O.V., Vysokomornyi, V.S., Strizhak, P.A., 2013. Estimation of reliability parameters of operation of autonomous devices for energy saving in remote linear objects of long-range pipelines of eastern siberia and far east. Izv. Tomsk. Politekh. Univ. 4, 59–65.
Wen, X., Luo, K., Luo, Y., Kassem, H.I., Jin, Hanhui, Fan, J., 2016. Large eddy simulation of a semi-industrial scale coal furnace using non-adiabatic three-stream flamelet/progress variable model. Appl. Energy 183, 1086–1097.
Xin, Y., Clements, A., Szuhánszki, J., Xiaohong, H., Moguel, O.F., Jia, L., Gibbins, J., Zhaohui, L., Chuguang, Z., Ingham, D., Ma, L., Nimmo, B., Pourkashania, M., 2018. Prediction of the radiative heat transfer in small and large scale oxy-coal furnaces. Appl. Energy 211, 523–537.
Zakharevich, A.V., Kuznetsov, G.V., Salomatov, V.V., Strizhak, P.A., Syrodoy, S.V., 2016a. Initiation of combustion of coal particles coated with a water film in a high-temperature air flow. Combust. Explos. Shock Waves 52, 550–561.
Zakharevich, A.V., Salomatov, V.V., Strizhak, P.A., Syrodoi, S.V., 2016b. Ignition of the drops of coal–water fuel in a flow of air. Solid Fuel Chem. 50 (3), 163–166.
Zhang, Y., Wu, Y.Yu.Bo., Wu, X., Huang, Z., Zhou, J., Cen, K., 2014. Flow behavior of high-temperature flue gas in the heat transfer chamber of a pilot-scale coal-water slurry combustion furnace. Particuology 17, 114–124.